University of Groningen

Studies of fullerenes by the excitation, emission, and scattering of electrons

Rudolf, Petra; Golden, M.S.; Bruhwiler, P.A.

IMPORTANT NOTE: You are advised to consult the publisher's version (publisher's PDF) if you wish to cite from it. Please check the document version below.

Document Version
Publisher's PDF, also known as Version of record

[Link to publication in University of Groningen/UMCG research database](#)

Studies of fullerenes by the excitation, emission, and scattering of electrons

Petra Rudolf[a,*], Mark S. Golden[b], Paul A. Brühwiler[c]

[a]*Laboratoire Interdisciplinaire de Spectroscopie Electronique, Facultés Universitaires Notre-Dame de la Paix, Rue de Bruxelles 61, B-5000 Namur, Belgium*
[b]*Institut für Festkörperforschung, IFW Dresden e.V., PO Box 270016, D-01171 Dresden, Germany*
[c]*Department of Physics, Uppsala University, Box 530, S-75121 Uppsala, Sweden*

Abstract

This paper presents an overview of how electron spectroscopies have contributed to advances in fullerene research. In particular, we illustrate the vital role these techniques have played in improving our understanding of the importance of strong electronic correlation and of electron-phonon coupling in these materials, in the derivation of electron hopping rates, in providing a direct determination of charge transfer and hybridisation in both fullerene salts and adsorbed fullerenes and in determining the optical gap of these systems. We discuss systems of increasing complexity, starting with C_{60} in the gas phase and in the solid state, and moving on to C_{60} salts and to C_{60} adsorbed on surfaces. Finally we look at both higher fullerenes and fullerenes with a heteroatom either on or inside the cage. © 1999 Elsevier Science B.V. All rights reserved.

1. Introduction

Over the past decade, the fullerenes have been the subject of scientific scrutiny on a scale unprecedented in research into conjugated carbon-based systems. The reasons for this are two-fold. Firstly, the fullerenes and their compounds exhibit an extremely rich collection of interesting and potentially useful physical properties: they are excellent electron acceptors, can be transformed into synthetic metals, exhibit superconductivity at transition temperatures only exceeded by those of the cuprates, support ferromagnetism (without the presence of d or f electrons) and display remarkable non-linear optical

behaviour. However, arguably as important as their properties is the fact that fullerenes in general, and C_{60} in particular, possess extremely high symmetry. This point goes far beyond their aesthetic appeal to the human desire for structural symmetry, and in fact allows access to an experimental and theoretical understanding of a large-scale molecular system on a extraordinarily fundamental level. Taking these two facets of fullerene science together, one can understand why C_{60} has become the conjugated carbon-based molecule par excellence, a system whose properties can be systematically followed from the gas phase, via ultra-thin films adsorbed on surfaces, to solid state compounds.

With these points in mind, electron spectroscopies present themselves as ideal tools with which to study both the electronic and vibrational properties of these systems with parallel analysis of their molecular and

*Corresponding author. Tel.: +32-81-725-237; fax: +32-81-724-595.

E-mail address: petra.rudolf@fundp.ac.be (P. Rudolf)

solid-state structure. In this review, we aim to illustrate the central role which has been played by electron spectroscopies in fullerene research up to the present. For more exhaustive accounts of the spectroscopic aspects of both surface related and solid state fullerene research, we refer the reader to Refs. [1–5]. To give the reader an idea of the breadth over which electron spectroscopy has made an impact, some of the landmark contributions are listed below:

- Direct photoemission spectroscopy (PES), inverse photoemission (IPES) and X-ray absorption (XAS)
  - the role played by strong electronic correlation
  - the importance of electron-phonon coupling
  - direct determination of charge transfer and hybridisation
  - derivation of phase diagrams for the fullerene salts
  - local structural information

- Resonant photoemission (RESPES) and Auger electron spectroscopy (AES)
  - the role played by strong electronic correlation
  - determination of hopping rates

- Electron energy loss spectroscopy (EELS)
  - determination of optical gaps and exciton binding energies
  - vibrational characterisation at surfaces
  - the role played by strong electronic correlation in the intercalated systems

In the main body of the review, examples of many of the points listed above will be given, presented upon a framework of increasing structural complexity, starting with gas phase data, going on to the solid state and intercalated compounds, including adsorption and doping of C_{60} on surfaces, and finally touching on some of the more exotic systems such as the higher fullerenes, endohedral and heterofullerenes.

Taken in its entirety, the major contribution made by the electron spectroscopic investigation of these materials can be summed up as an awareness that the physics and chemistry of these molecules and their compounds goes far beyond that of pristine or doped carbon-based semiconductors. The view that has emerged from the efforts of the community over the last ten years is rather that these fascinating materials are more correctly described as narrow band, strongly correlated Jahn-Teller systems.

2. C_{60} in the gas phase

Before C_{60} or other fullerenes were available in macroscopic quantities, electron spectroscopic studies of these molecules were being conducted on molecular beams. Fig. 1 shows the two important quantities which can be obtained directly from gas phase electron spectra: the ionisation potential (IP) and electron affinity of C_{60}. A vertical IP of about 7.75 eV [6–8] can be estimated from photoelectron spectra of neutral C_{60} (which gives C_{60}^{+} in the final state). The adiabatic IP is closer to 7.54 eV as measured by photoionisation yield [9], which is also supported by analysis of the vibronic structure in high-resolution PES data [7]. Comparisons of these values to other techniques are given elsewhere [10]. PES of the negative ion (giving a neutral C_{60} final state) determines the electron affinity (EA) to be about 2.80 eV [11–13] and the intrinsic energy separation (Δ) between the h_{u} (highest occupied molecular orbital – HOMO) and the t_{1u} (lowest unoccupied molecular orbital – LUMO) to be 2 eV [14]. The IP and EA values make it clear that one would expect C_{60} to be a good electron acceptor and a poor donor, a conclusion which has been borne out in many experiments. The energy IP$-$EA$-\Delta$ defines the on-ball Coulomb interaction, U, thus giving a value to U of the order of 3 eV for the free molecule.

A representative wider-range gas phase PES spectrum [6] is shown in the left side of Fig. 2. One can immediately get a sense of the high degree of orbital degeneracy which is the hallmark of C_{60}: although the system has 60 π-electrons, PES shows only a handful of peaks at low binding energy. It is in fact relatively straightforward [15] to correlate the features in the photoemission spectrum with the different molecular orbitals (MOs) of icosahedral C_{60}. The states nearest to the chemical potential are derived
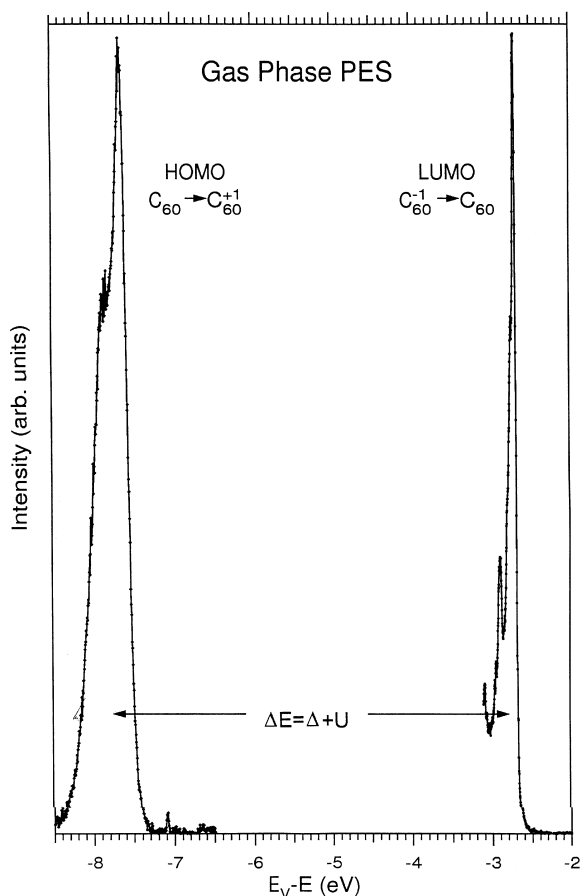
Fig. 1. Gas phase PES data of the indicated levels from neutral and negatively-charged free C_{60} (the term LUMO refers here to the ground state of the neutral molecule), from Refs. [7,11]. See the discussion in the text for interpretation of the energy difference and spectral widths.

from the h_{1u} HOMO. The peak which comes next in energy is due to both the h_g and g_g states and is generally referred to as the HOMO-1. Both the HOMO and the HOMO-1 are pure π-MOs [15]. The features at higher energy result from the overlap of both π and σ-MOs. Recent work [16,17] has shown that the cross sections of these peaks vary due to interference effects arising from the shell-like structure of C_{60}.

The right side of Fig. 2 shows the corresponding C 1s excitation spectrum of matrix-isolated C_{60}, measured using XAS [18,19], and placed on a common binding energy scale. This was done by subtracting the photon energy from the gas phase C 1s IP. The

latter was determined from the C 1s IP of solid C_{60} as in Refs. [20,21], using the gas phase-to-solid state screening shift for the HOMO band. However, since the shift taken there uses the peak in the gas phase HOMO band at 7.61 eV instead of the centroid at 7.75 eV, the experimental screening shift should not be 0.7 eV as given there, rather ~0.85 eV, which is what we use here. This results in a predicted gas phase C 1s IP of 290.45 eV. The next point to consider is that the photon energies of the different XAS transitions are virtually the same for solid, gas, and matrix-isolated phases [18,19], so that calibrating the matrix-isolated XAS data in this way should give an accurately calibrated final result. As seen, the XAS spectrum is dominated by sharp π* resonances, the first pair of which can be considered to be transitions into the t_{1u} and t_{1g} MOs (or LUMO and LUMO+1), modified by the presence of a core hole [22]. The high symmetry is seen again via the relatively sharp and sparse peaks in the spectrum (the shaded peak is due to CO frozen into the Xe matrix). As seen here, XAS is a technique that allows one to access the unoccupied levels without a convolution over occupied states (the first level is available via PES [11]). Since the C 1s IP gives the electron removal threshold in the spectra, the spectrum calibrated in this way represents the energy required to ionise a core-excited molecule, and thus is quite similar to PES energetically (note that the correlation energy of a positive hole is common to both spectra). The main difference is that the core hole can enhance, e.g., the LUMO binding energy due to the precise distribution of the wave function, which should be an effect of the order of 0.2–0.3 eV [18,19,22]. Thus the HOMO-LUMO separation ΔE~ 1.8 eV, shown in Fig. 2, is very close to the true singlet gap of ~2.0–2.2 eV [23]. The small difference is just the core hole effect, which is difficult to measure precisely due to the difficulty of determining the singlet gap energy and the gas phase C 1s IP, but which appears to be of the expected magnitude.

There have also been EELS measurements of C_{60} in the gas phase [24–28], which, apart from revealing low-energy interband transitions, also show collective excitations such as the π- and σ-plasmons [29], as do photo-ion yield studies [9].

Valuable information on vibrational coupling can be obtained from high-resolution PES measurements on cooled, negatively-charged C_{60} beams [11]. These
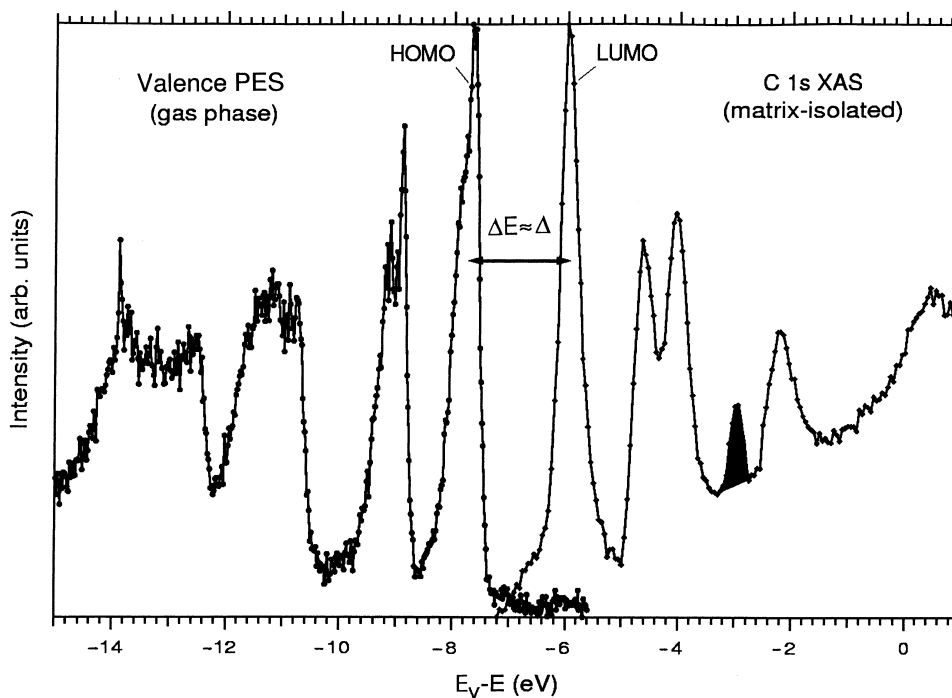
Fig. 2. Gas phase PES [6] compared to matrix-isolated C 1s XAS data [18,19] for C_{60}. The data are placed on a common binding energy scale (E_v=vacuum level) as described in the text.

data, combined with sophisticated calculations [11], are the only direct measure of the parameters employed in the most common model of superconductivity in the alkali-fullerides (to which we return in Section 4). For C_{60}^-, the triply-degenerate LUMO is the level in which the single charge resides, and it will couple to all of the H_g vibrations via the Jahn-Teller effect, which breaks the electronic degeneracy to lower the total energy [11,30]. Analogous data for C_{60}^+, as measured in PES on neutral beams [7], suggest that the vibrational-electronic (vibronic) coupling to a vacancy, or hole, in the HOMO is even stronger than the coupling to an electron in the LUMO. This difference in coupling strengths between the case of final states with a hole in the HOMO (PES of C_{60}) and the neutral LUMO (PES of C_{60}^-) can be seen by eye in Fig. 1.

It is possible to obtain a stable higher charge state on the C_{60} cage in the gas phase, but only by forming a complex with, e.g., alkali atoms that readily donate their single valence charge. A study of this by PES in the gas phase has been carried out

[31], showing that it is possible to achieve high levels of charge transfer in this manner, with an electronic structure quite reminiscent of that of C_{60}^-, as expected for a simple charge-transfer-bonded complex. Effects of alkali-C_{60} vibrations were also detected in the spectra. The fact that the electron affinity tends monotonically towards 0 eV with increasing K 'coverage', indicates an electronic limitation on the extent to which charge transfer can be expected to explain the bonding of K to C_{60}, a topic which has been studied further in films (Section 4).

3. C_{60} in the condensed phase

The nearly-spherical structure and large size of C_{60} comprise a unique structural unit for condensed materials. In the solid at 300 K, the C_{60} molecules rotate very rapidly (they are in fact more labile than in solution), resulting in a lattice with *fcc* symmetry and a lattice constant of $a_0 = 14.2$ Å [32,33]. Below

~260 K there is a first order phase transition from *fcc* to an orientationally ordered simple cubic (*sc*) phase (the icosohedral point group symmetry of the C_{60} molecule is incompatible with a rotationally ordered *fcc* phase). The C_{60} molecules, however, continue to 'ratchet' from one preferred orientation to another. This rotation is finally frozen out on crossing a glass transition at ~90 K, which leaves ~85% of the C_{60} molecules in one orientation and the remaining 15% in another orientation of slightly higher energy [34]. These structural properties are, in general, consistent van der Waals bonding (as expected for spherical graphitic molecules) [35], and suggest that the electronic and vibrational states should be closely related to those of the isolated molecule. This is found to be the case, but there are interesting and non-trivial properties which emerge in studying pure fullerite with electron spectroscopies.

Looking at Fig. 3, which shows both the PES [36] and IPES [37] spectra of a thin, crystalline film of C_{60} on Au(110), and comparing it to the gas phase data of Fig. 1, one can see that there is a strong similarity between the electronic structures of free and condensed C_{60}. A broadening of all levels is observed in the solid. The energy separation of the HOMO in electron removal and the LUMO in electron addition is ~3.5 eV [4,38] (peak to peak).

This is the energy gap of solid C_{60} relevant for determining transport properties. Comparing this value with the gas phase data above, one can conclude that the effective Coulomb interaction is reduced due to the effects of long-range screening [39], which in this case involves the dielectric screening of both charges (i.e. the hole in the HOMO in PES and the electron in the LUMO in IPES). Calculations of this screening agree that it amounts to slightly more than 0.8 eV for each charge [40–42], giving a total of ~1.6 eV reduction in U from the gas phase value of 3 eV (see above) to ~1.4 eV. This value can be checked independently by comparing Auger and PES data [40,43,44], as shown in Fig. 4. There the Auger, with a smooth component removed to reveal the fine structure, is plotted with the self-convolution of the PES spectrum. Since Auger creates a two-hole final state (necessarily on the same molecule), whereas photoemission creates a one-hole final state, the self-convolution of PES is a reasonable approximation to the two-hole energy spectrum for the case where the holes are on different C_{60} molecules. This is seen to be the case in the figure, with the exception of an energy shift of ~1.4 eV needed to align the spectra; indeed, the self-convolution gives a good approximation to the unmanipulated Auger spectrum [45]. This required
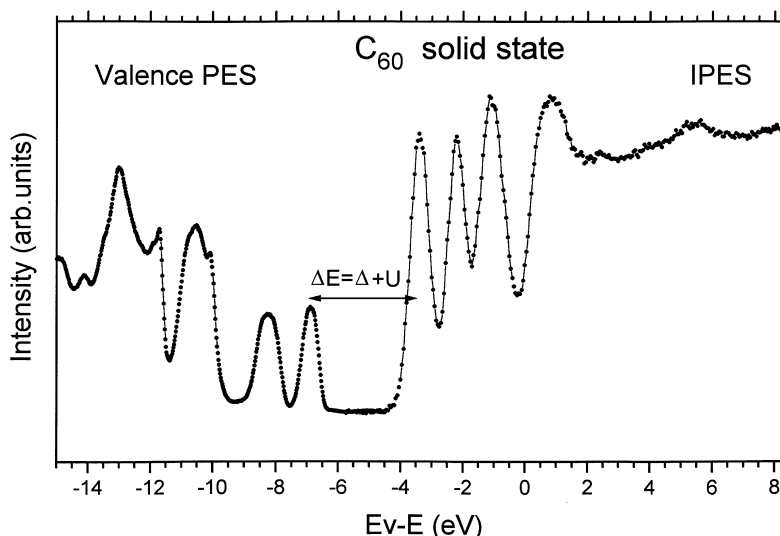

Fig. 3. PES [36] and IPES [37] data of thin multilayer films of C_{60}/Au(110), placed on a common energy scale (E_v=vacuum level) in analogy to Fig. 1.
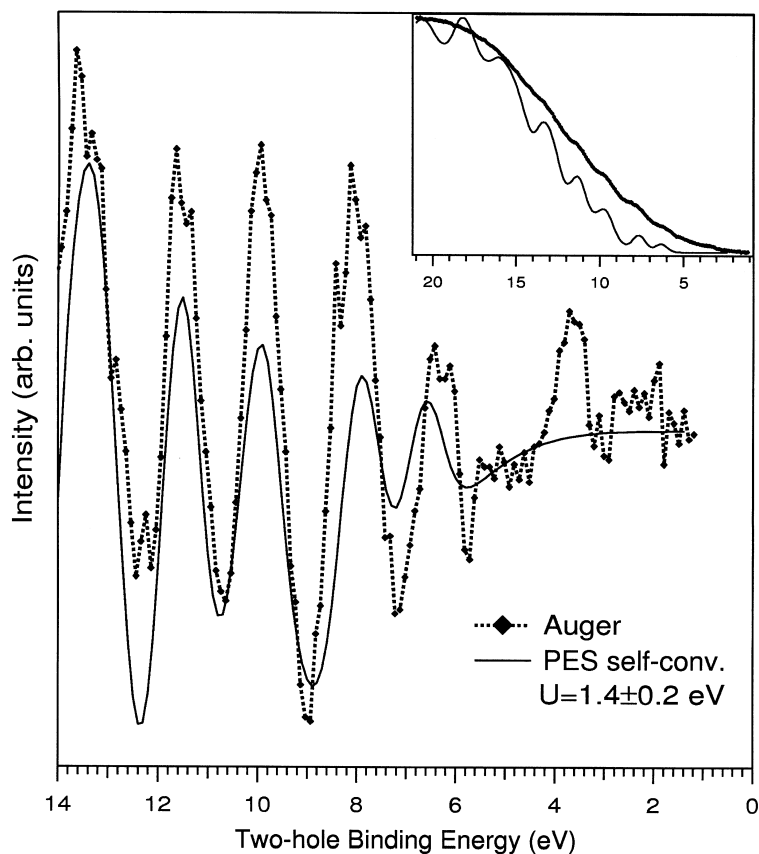
Fig. 4. Auger intensity oscillations compared to those of a self-convoluted PES spectrum in order to estimate U in solid C_{60} [43]. The inset shows the raw data and self-convolution.

shift is just U, here detected as an intramolecular hole-hole interaction. A closer examination indicates that U varies with the final state, corresponding to subtleties in the details of the intramolecular Coulomb interaction with charge distribution, which has been discussed in more detail elsewhere [44,46,47].

Another aspect of the reduction of U in the solid is the surface core level shift. Because the dielectric screening varies between surface and bulk, so does the screening shift observed in PES. The observed [41,48] shift of ~0.1 eV for the C 1s level is consistent with numerical estimates [41,42]. To understand this, however, it was vital to note that a 1s vacancy is screened internally by the molecule in

such a manner as to redistribute the net charge of $+1$ almost uniformly over the entire molecular surface [41]. A similar phenomenon is found to explain the lowest energy C 1s shake-up line [49], which establishes a characteristic for aromatic systems from benzene to graphite [50], and reflects a metal-like ability to screen internal charges.

It should be noted that at 1.4–1.6 eV U in solid C_{60} is larger than one-electron bandwidths ($W=0.5–1.0$ eV) near the HOMO-LUMO gap from LDA calculations [51,52], thus placing pristine solid C_{60} in the Mott-Hubbard regime ($U>W$) [40]. This fact also has consequences for the nature of its electronic excitations as can be seen in Fig. 5. Here we show EELS spectra for solid C_{60}, measured both in
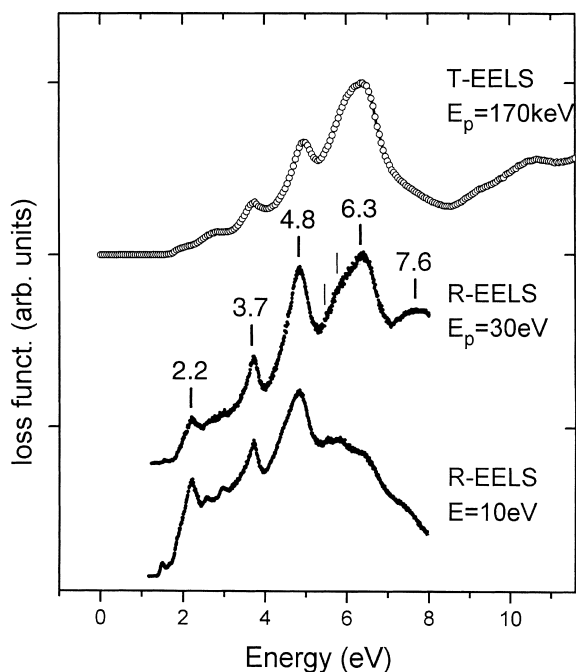
Fig. 5. EELS of solid C_{60} measured in both transmission [55,56] and reflection [53,54].

reflection [53,54] (E_p=10 eV and 30 eV), and transmission [55,56] (E_p=170 keV). For low primary energies, the first electronic excitation is located at 1.55 eV [53,54]. However, for high primary energies the first structure is at 1.8 eV. This illustrates that, rather than giving a measure of the 'band gap', these EELS experiments reveal the energy required to form on-ball (Frenkel) excitons [40,42,57]. The lowest lying excitation is the $^3T_{2g}$ triplet state [58,59], with the higher energy feature representing the corresponding singlet. This first pair of features arise from $h_u \rightarrow t_{1u}$ transitions and are thus formally dipole forbidden. This tallies with the observed q-dependence of the spectral weight at 1.8 eV in EELS in transmission studies [60,61].

However, the fact that the triplet exciton energy shows a slight temperature dependence [62], does imply that this excitation possesses some degree of delocalisation. Furthermore, this temperature dependence can be used to show that the outermost surface

layer in C_{60} undergoes the high temperature orientational phase transition at temperatures ~35 K lower than the bulk [62].

As we consider the EELS spectra of Fig. 5, going to higher loss-energies, apart from a number of transitions between individual π and π^* MOs (interband transitions), the main feature is the so-called π-plasmon located at 6 eV, which results from the collective excitation of the complete π-electron system (i.e. all π–π^* transitions). EELS measurements as a function of momentum transfer show that the π-plasmon exhibits negligible dispersion [60,61], contrary to the behaviour observed for π-systems involving delocalised electronic states such as graphite [63], or single-wall carbon nanotubes [64]. At still higher energies (not shown), there contribute interband transitions involving the σ^* manifold of MOs and the ($\pi+\sigma$)-plasmon is observed at around 25 eV [53–56], as was the case in the gas phase.

Both angle resolved direct (ARPES) and inverse photoemission (KRIPES) have been applied with the aim of determining the dispersive bandwidth in solid C_{60}. In the ARPES data, the dispersion is dominated by that of the unoccupied states [5,65–67], whereas the KRIPES data showed minimal dispersion [68]. Thus there has been no direct experimental confirmation of band dispersions on the order of the theoretical bandwidth estimates [51,52]. On the other hand, PES data for a monolayer of C_{60} on graphite compared to gas phase data indicate vibronic effects could well account for a large fraction of the observed solid state bandwidths, and that screening effects [41] complicate the data analysis considerably [7].

The comparison of RESPES and XAS data of solid and matrix-isolated C_{60}, shown in Fig. 6, illustrates nicely both sides of the 'bandwidth' coin. RESPES spectra show that there exists a significant intermolecular hopping pathway for electrons in the close-packed C_{60} solid [18,19]. On the other hand, the XAS data illustrate that the vibronic coupling, which explains the linewidths in the spectrum of the isolated molecule, remains undiminished in the solid phase spectrum [18,19]. In particular, as the first XAS resonance lies in the fundamental gap, it can essentially only be vibronically broadened. In this respect, solid, pristine C_{60} is an excellent testbed for
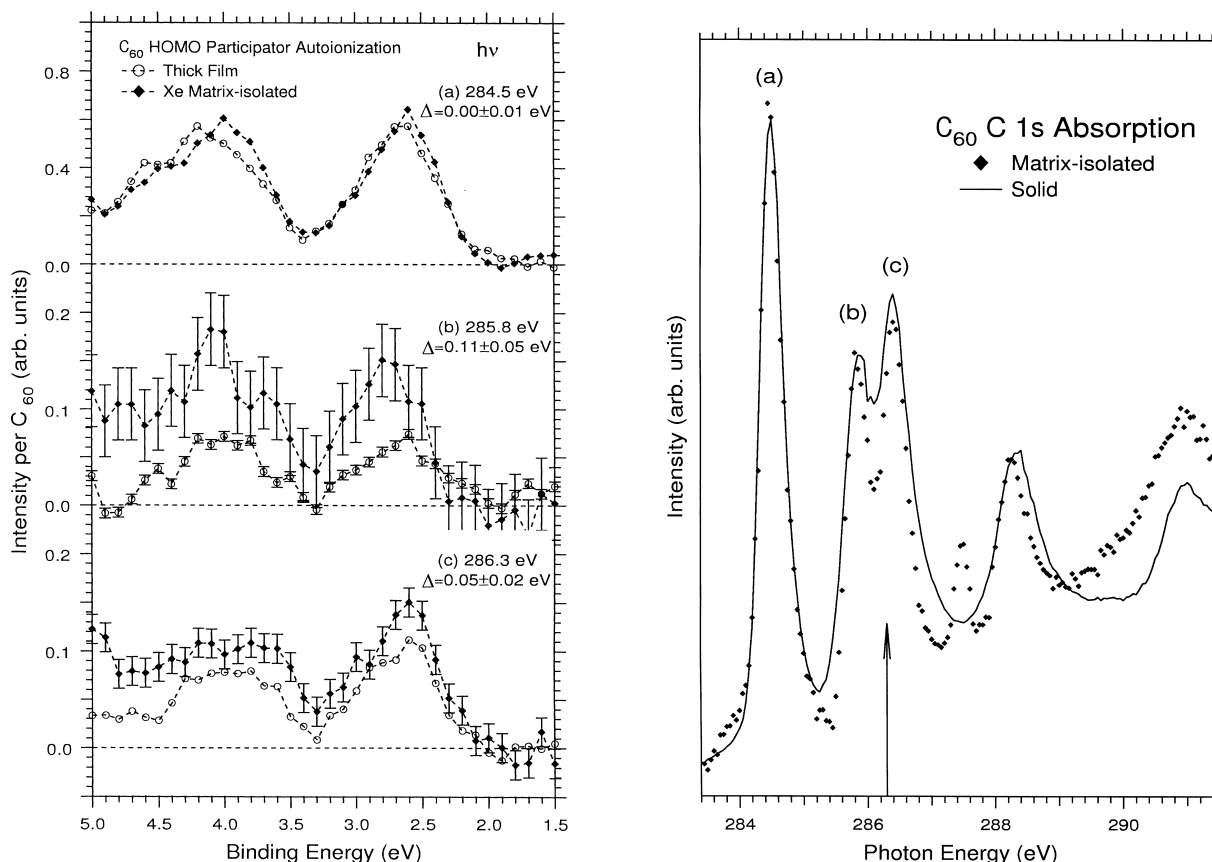
Fig. 6. RESPES and XAS data comparing matrix-isolated to solid C_{60} for the extraction of bonding effects [18,19].

our understanding of the interplay between electronic and vibronic (i.e. polaronic) properties for such large systems [7].

4. Intercalated C_{60} in the solid state

C_{60} forms compounds with the alkali or alkaline earth metals leading to A_xC_{60} salts. In general, these salts involve the occupation of the interstitial sites of the C_{60} lattice by the cations. For *fcc* C_{60}, two tetrahedral and one octahedral site per molecule are available for intercalation. The extreme variation in the physical properties of intercalated C_{60} compounds makes the investigation of their electronic and vibrational characteristics of great interest. Fig. 7 shows one of the early combined PES/XAS studies of thin films of K_xC_{60} obtained by successive

intercalation of C_{60} in UHV [69]. Electron spectroscopies offer a direct way of determining the charge state of the C_{60} molecules, for example showing clearly that the highest possible intercalation stage of six results in complete filling of the LUMO-derived states (i.e. $(C_{60})^{6-}$), and that for intermediate doping a clear Fermi edge signals the presence of a metallic phase. Fig. 8 illustrates that $(C_{60})^{6-}$ does not necessarily represent a limit for the maximal charge state. In this case, C_{60} has been deposited at sub-monolayer (ML) coverages on a thick K film [70], which results in PES and XAS spectra consistent with a metallic fulleride system with a C_{60} charge state of ca. -11, leading to near complete filling of the t_{1g} (LUMO+1)-derived states. For increased C_{60} coverage, a series of non-metallic systems results until eventually K_6C_{60} is reached. In general, the intercalation behaviour of the
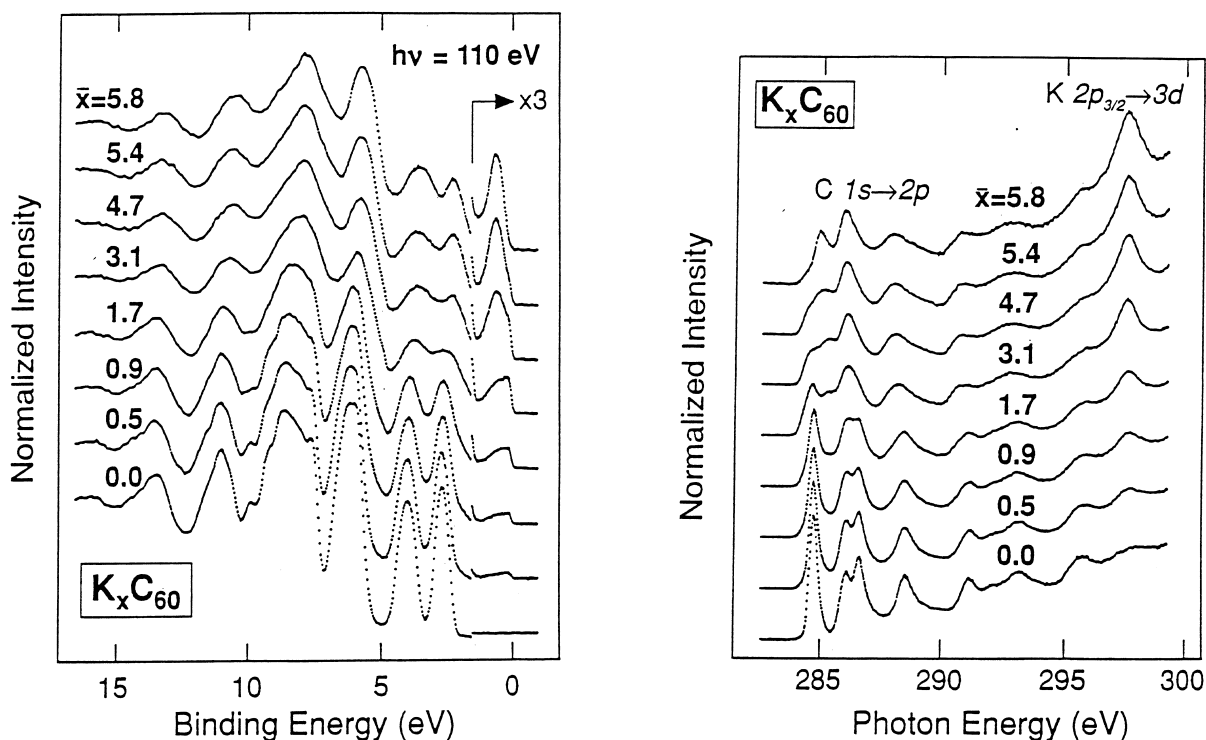
Fig. 7. PES and XAS of K_xC_{60} [69] for successive intercalation of K into C_{60}.

heavier alkali metals (Rb, Cs) with C_{60} is very similar to that of K. For the case of Na, its small size results in multiple occupancy of the octahedral site, with interesting results for the electronic structure. Fig. 9 shows a series of C 1s excitation spectra of the Na_xC_{60} system recorded using EELS in transmission [71]. Up to Na_6C_{60}, the C_{60} charge state increases linearly with doping. However, as can be seen in the inset, between $x=6$–8, the charge state of the fullerene remains constant, before once again increasing to a maximum of $(C_{60})^{10-}$ for $Na_{12}C_{60}$. This pause in the charge transfer is a direct consequence of the formation of a fully ionised Na-aggregate around the octahedral site, giving rise to an 'O void' with an attractive potential for electrons [71,72]. The 'O' state has neither pure Na 2s nor C_{60} character and is populated by 2 electrons before further intercalation leads to the onset of the filling of the C_{60} t_{1g}-derived states. Further systems in which the t_{1g} levels of C_{60} become populated are the Ca or Ba fullerides. Here PES [73,74], EELS in transmission [75] and RESPES [76] investigations

could show clearly that there exists strong hybridisation between the electronic states of the alkaline earth and the C_{60}.

In order to be able to investigate the electronic and geometrical structure of the different C_{60} compounds in detail, it is vital to be able to control the phase purity of the samples. Crucially, it was shown early on that core level BE shifts between the intercalant ions situated at the tetrahedral and octahedral sites provide a highly effective monitor of phase purity of fulleride samples prepared in UHV [77]. This led to the development of recipes allowing the preparation of phase-pure fulleride samples via vacuum distillation of multiphase intercalated C_{60} [78,79].

Fig. 10 shows transmission EELS data from distilled, phase-pure samples of K_xC_{60} ($x=0, 3, 4, 6$) [5,80]. EELS in transmission possesses the additional advantage that by setting the loss energy to zero, electron diffraction studies can be carried out in situ, allowing a further characterisation of the phase purity of the samples under investigation. The energy range displayed (up to 2 eV) contains only features
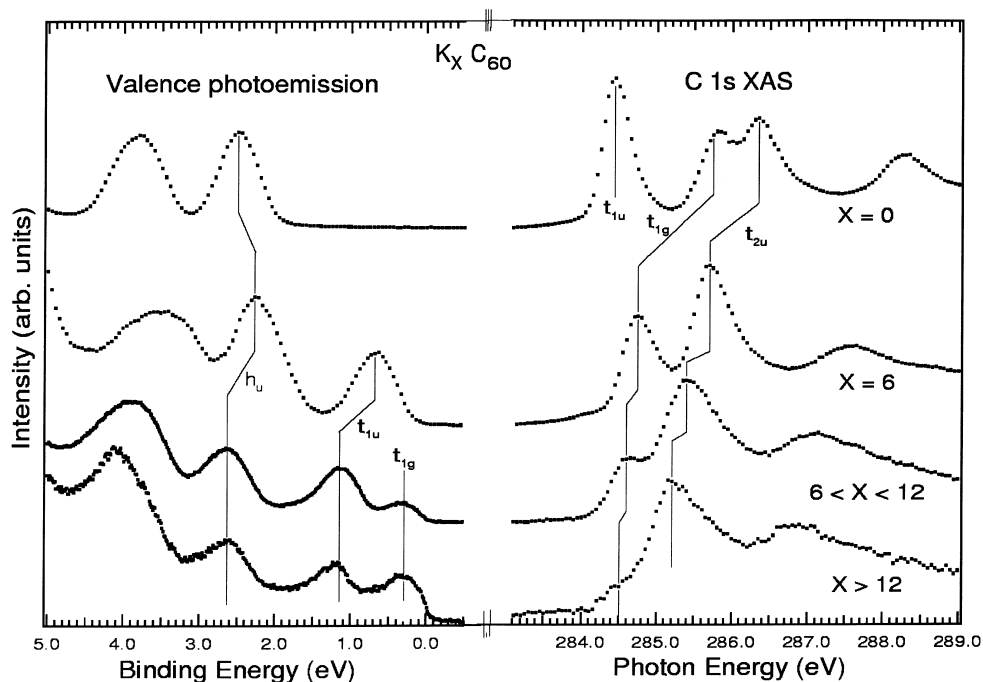
Fig. 8. PES and XAS of K_xC_{60} [70] for successive evaporation of C_{60} onto a K multilayer.

related to the low energy intra- and inter-band ($\pi \rightarrow \pi^*$) excitations. K_6C_{60} shows a single, strong, asymmetric peak located at 1.35 eV resulting from dipole allowed $t_{1u} \rightarrow t_{1g}$ interband transitions [5]. The loss of function of K_4C_{60} also indicates an insulating ground state for this system [81,82], which is contrary to the expectations from a rigid-band picture for doping in which the LUMO-derived band would be $\frac{2}{3}$ filled. The scenarios proposed to explain this observation have included the suggestion of a Mott-Hubbard ground state [40,83] for A_4C_{60}, or a description of these compounds as Jahn-Teller insulators [84,85]. The EELS loss of function of K_4C_{60} is comprised of four features (two strong, two shoulders). As only $t_{1u} \rightarrow t_{1g}$ transitions are possible in this energy range, this indicates that these MOs are split in this material [80,86]. Further information can be derived from an analysis of the optical conductivity of different A_4C_{60} compounds (derived from Kramers-Kronig transformation of the loss function) as well as of $Na_{10}C_{60}$ (which has $\frac{1}{3}$ filled t_{1g}-derived states [71]), which is shown in the left-hand panel of Fig. 11 [87]. The right-hand panel of

the same figure contains an analysis of the data in terms of a Lorentz model, enabling the extraction of the energy of the first transition as a function of the inter-C_{60} spacing in the different crystal structures (shown as symbols). Unlike the transitions at higher energies, this first transition clearly depends upon the intermolecular distance, and thus can be attributed to the intermolecular 'gap' transition. The d-dependence of this transition is well reproduced by a simple Mott-Hubbard model [87], shown as solid lines in the right-hand panel of Fig. 11. Thus, the insulating nature of the A_4C_{60} systems is a result of the strong electronic correlation prevalent in C_{60}, as discussed in Sections 2 and 3. However, the fact that the data of Figs. 10 and 11 clearly show at least three features are consistent with a Jahn-Teller distortion of the $(C_{60})^{4-}$ (or $(C_{60})^{8-}$) molecules and the consequent splitting of the t_{1u} and t_{1g}-derived electronic levels [86,87].

Apart from in the EELS data discussed above, the impact of electron correlation in the A_xC_{60} system can also be illustrated using the PES/IPES spectra [88] of vacuum distilled, phase pure C_6C_{60}, shown in
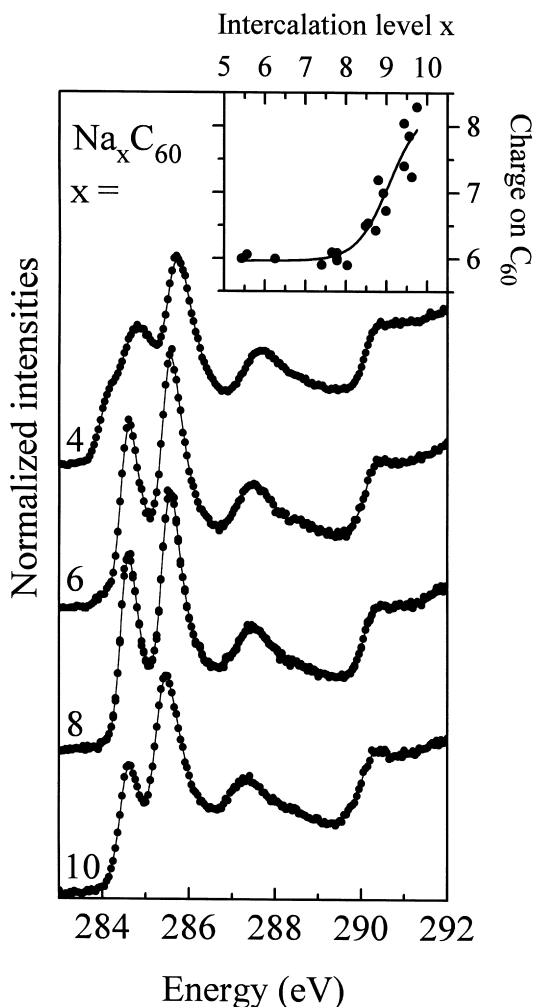
Fig. 9. Transmission EELS data at the C 1s edge for Na_xC_{60} [71]. The inset shows the charge state as a function of x derived from the t_{1g}-derived spectral weight.

Fig. 10. The loss function of phase-pure K_xC_{60} measured using EELS transmission [5].

Fig. 12. The energy scale is referenced to the vacuum level [20,21,89]. The peak to peak energetic separation of the t_{1u} and t_{1g}-derived spectral features, which measures the solid state equivalent to the gas phase IP−EA, is 2.6 eV. Under the assumption of rigid band filling, this quantity may be compared with the energy separation of $\Delta=1.2$ eV in the IPES of solid C_{60} (Fig. 3). These numbers imply that $U=1.4$ eV, which is in good agreement with the results of Auger/PES investigations of K_6C_{60} [43]. An analogous analysis of the data for Cs_4C_{60} leads to a similar value of $U\simeq1.5$ eV [89].
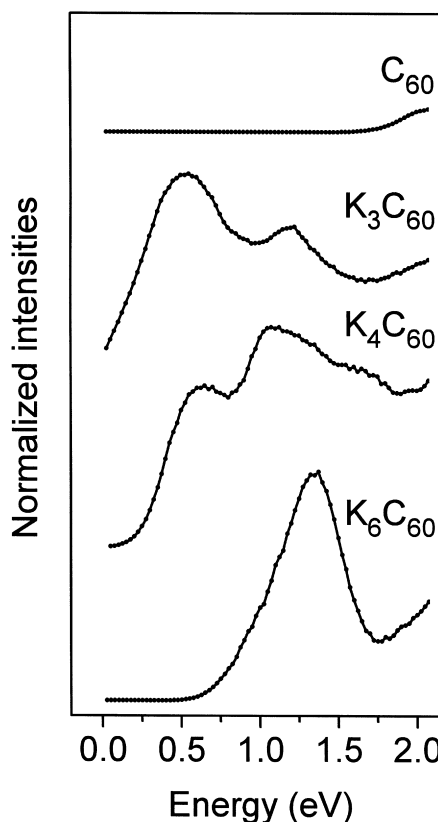
We begin our discussions of the A_3C_{60} materials by returning to Fig. 10. The loss function of K_3C_{60} contains two low energy features: at 0.55 eV is a combination of the plasmon associated with the t_{1u} charge carriers and transitions within the three t_{1u} sub-bands [90], the $t_{1u}{\rightarrow}t_{1g}$ transitions appearing at 1.2 eV. Momentum dependent EELS investigations [91] have shown that the 0.55 eV plasmon (whose width of 0.5 eV is a result of electron-phonon interactions [92]), is essentially dispersionless, which disagrees with theoretical predictions of a negative plasmon dispersion due to local crystal field effects [93]. In fact, these effects are exactly cancelled out by the reduced screening of the plasmon by interband transitions at higher q [91].

The 0.55 eV plasmon also makes itself felt in high resolution PES studies of A_3C_{60} [94,95]. The bottom panel of Fig. 13 shows the PES profiles of the
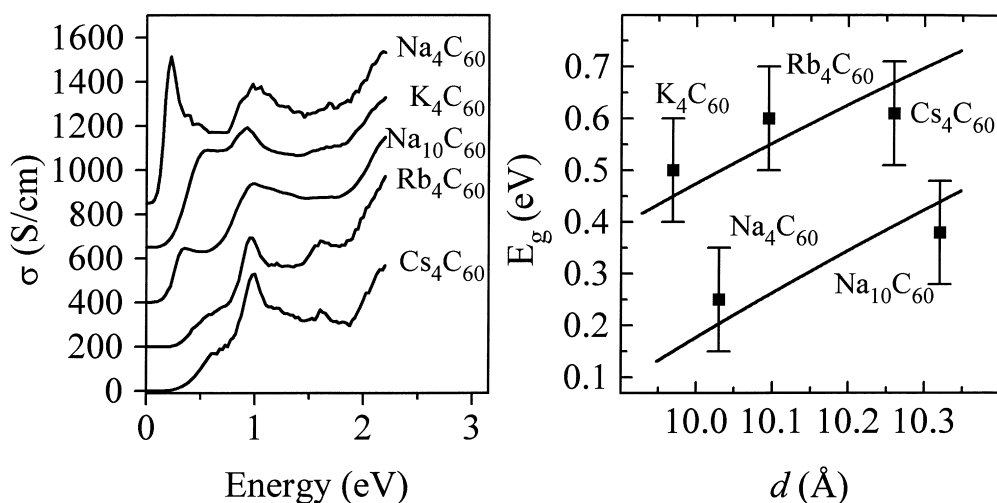
Fig. 11. Left panel: Optical conductivity of phase pure A_4C_{60} and $Na_{10}C_{60}$ derived from a Kramers-Kronig analysis of transmission EELS data. Right panel: The experimentally determined energy gap as a function of the nearest neighbour separation. The solid lines show the expected behaviour for *fcc* (lower line) and *bct* (upper line) phases within a simple Mott-Hubbard model [87].

LUMO-derived states of K_3C_{60} and Rb_3C_{60} recorded at T=15 K [94]. The width of the LUMO-derived states (more than 1.2 eV) deviates remarkably from that of 'half' of the t_{1u}-derived states in the PES of the A_6C_{60} systems shown in Figs. 7 and 12, which would give a t_{1u}-derived linewidth for

Fig. 12. PES and IPES data for phase pure Cs_6C_{60} [88]. The combination of these data with those for pure C_{60} of Fig. 3 is used to determine U, as described in the text.

A_3C_{60} of ca. 0.7 eV. The fine-structure near the sharp Fermi cut-off is a clear signal of the same kind of vibronic effects as were discussed in the context of the gas phase PES data shown in Fig. 1. Also in the bottom panel of Fig. 13 are PES calculations for A_3C_{60} confirming that good agreement with experiment can indeed be found by taking into account relatively strong coupling of the electronic system to the molecular A_g and H_g modes together with coupling to the 0.55 eV charge carrier plasmon discussed above [94]. While the role of vibrons in the PES of A_3C_{60} is undisputed, there is an alternative interpretation of the spectral weight at higher energies (0.5–1 eV) in terms of a correlation-induced satellite [95–97]. One approach to investigate this question is to look at ultra-thin films on metallic substrates such as are discussed in Section 5. This strategy is based upon the idea that systems such as 1 ML of K doped C_{60} on Au or Ag surfaces should have a reduced Coulomb interaction resulting from image charge screening [1,98,99]. The upper panel of Fig. 13 shows the PES spectrum of a 1 ML K_3C_{60} film on Au(110) [100]. The PES spectral weight in the energy region of the plasmon or correlation satellite appears to be strongly reduced in the surface compound. This result would seem to lend support to the correlation scenario, although the substrate-ful-
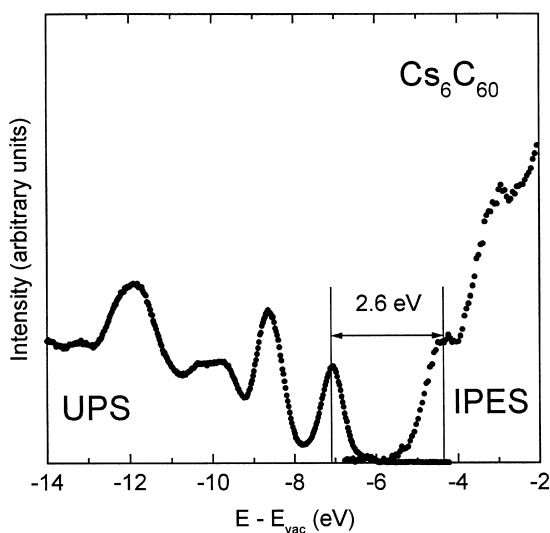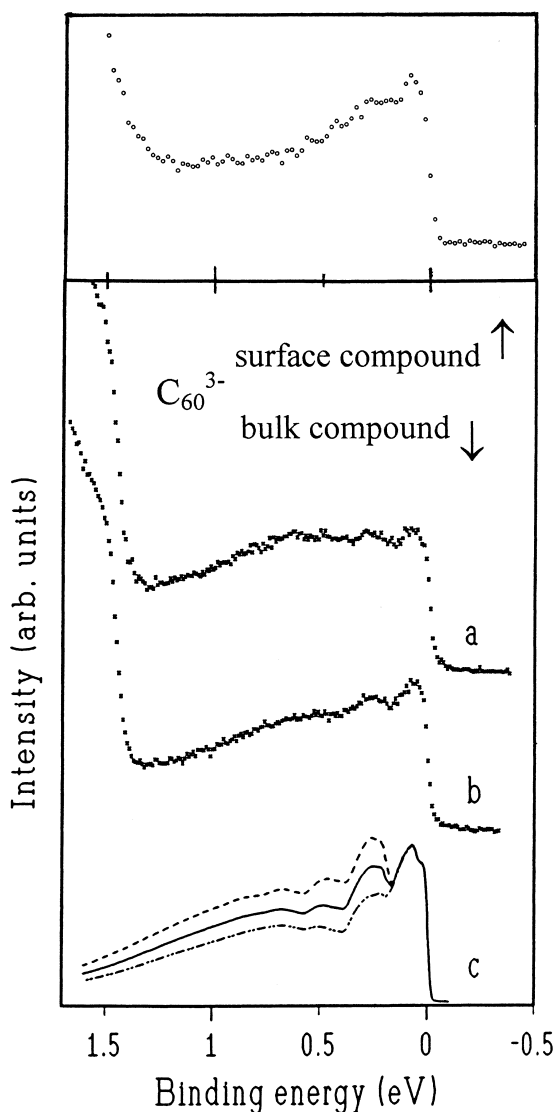
Fig. 13. High-resolution PES spectra of (a) K_3C_{60} and (b) Rb_3C_{60}, recorded at 15 K, compared to (c) a model spectrum including coupling both to intramolecular vibrations and the charge carrier plasmon [94]. Upper panel: PES spectrum of 1 ML K_3C_{60}/Au(110) [100].

lerene interaction is by no means limited to a mere screening of U, as will be amply demonstrated in Section 5 below.

The A_1C_{60} family were also a topic of interest for electron spectroscopists. Using distillation methods [77], and with knowledge of the rich phase diagram, it was possible to study all three known primary

phases of Rb_1C_{60} using valence photoemission: high-temperature rocksalt, stable polymer, and quenched dimer. Each phase showed a characteristic near-E_F electronic structure, varying from metallic, semimetallic, to insulating, respectively [101]. Similar PES structures (without phase purity, due to room temperature preparation) have been observed for Cs_1C_{60} [102–104], K_1C_{60} [102,103,105], Na_1C_{60} [103], and Li_1C_{60} [106], suggesting that this tendency is common to all the alkali metals. Calculations have shown that doping with one electron per fullerene lowers the barrier to polymerisation by the population of 'intermolecular' bonding orbitals [107].

Summing up this section, much of the information regarding electronic ground states of the A_3C_{60} and A_4C_{60} materials won using electron spectroscopies is consistent with a picture in which the former are just on the metallic side of a Mott transition, whereas the latter are just on the insulating side. This scenario receives support from theory in the form of the degeneracy-dependent Jahn-Teller contribution to the Coulomb interaction, which would tend to increase U in the A_4 systems, but decrease U in A_3 [108]. There is also growing experimental support for this picture: for example, A_4C_{60} can be induced to be metallic under pressure [109], and the expansion of the interfullerene spacing in the K_3C_{60} by ammoniation leads to the formation of an antiferromagnetically ordered insulator [110,111] (which itself can be driven metallic and superconducting by application of pressure).

5. C_{60} on surfaces

The adsorption of C_{60} on well-defined surfaces enables one to control the physical properties of the overlayer with a precision unmatched in bulk materials. This section aims to give a flavour of the defining role played by electron spectroscopies in the detailed characterisation of such systems. Firstly we deal with the strength of the fullerene-substrate interaction, and then the issue of charge transfer both at the surface and in novel two-dimensional A_xC_{60} compounds.

The interaction of C_{60} with different surfaces is not only of van der Waals type as originally thought

[112], and is actually observed on surfaces like GeS [113], SiO_2 [114], or graphite [7], but results in a great variety of both bond strength and bond character. On all metallic and conventional (Si, Ge, GaAs) semiconductor surfaces investigated so far [115], fullerenes are always chemisorbed, but the degree of hybridisation of the C_{60} molecular orbitals with the substrate electronic states and the amount of charge transfer differs greatly from substrate to substrate. The structure of the C_{60} monolayers is hexagonal or quasi-hexagonal resulting in compressed or enlarged C_{60}–C_{60} spacings compared to the C_{60} solid in order to achieve commensurate structures [1,2,115]. Photoelectron diffraction studies [116] showed that different adsorption geometries are possible for the chemisorption case, comprising a ring, a single or double bond of the C_{60} cage or even only a C_{60} edge atom facing the substrate, and that the adsorbed fullerenes do not rotate at room temperature.

Even for C_{60} MLs which are only physisorbed, PES has shown a slight change in the electronic properties of the molecule, namely a broadening of the valence band features [7,113] due to the symmetry reduction brought upon by adsorption which reduces the degeneracy of the molecular orbitals. In the case of polar substrates [113], a shift of substrate valence levels (band bending) attests to a polarisation of the adsorbed C_{60}. A chemisorptive interaction has been deduced from much more substantial changes in the PES, IPES and XAS data in which the spectral features derived from HOMO, HOMO-1, LUMO, LUMO+1 and LUMO+2 MOs (i.e. all orbitals with essentially π-character) change in width and shift in energy compared to their respective linewidths and positions in the C_{60} solid. The sensitivity of the individual shifts and broadening to overlap with substrate electronic states clearly points to the effects of hybridisation [1,2]. The spectral features associated with higher or lower lying MOs (including those which have significant σ character, as well as the C 1s level, e.g. Fig. 16 of Ref. [2]) show only rigid shifts and a slight broadening.

Additional information on the C_{60}-substrate interaction has been retrieved from the C 1s photoemission line and its shake-up satellites spectra such as those presented in Fig. 14 for a C_{60} multilayer and a ML grown on GeS(001), and a ML on Ag(111), Pt(111) and Ni(110), respectively [1,115]. All MLs except the one on GeS(001) show a shift in binding energy compared to the multilayer. It is difficult to extract quantitative information regarding charge transfer at the surface via comparison of C 1s BEs from ML and thick films. This is a consequence of the fact that many of the monolayers are metallic, whereas thicker films and van der Waals bound MLs are essentially insulators. This difference expresses itself in terms of the different energy references and screening contributions relevant to the two cases. Let us consider now the width of the C1s line. The intrinsic width for a thick film is measured to be of the order of 0.4 eV [117], which is much larger than the core hole lifetime broadening (~0.1 eV) [18,19]. The observed width can be attributed primarily to intrinsic electron-phonon coupling, as indicated by the similar width of the LUMO resonance in XAS, which, as discussed in the context of Fig. 6, is essentially only vibronically broadened. Within the Z+1 approximation, this broadening is purely a consequence of the symmetry-breaking due to the core hole [22], the magnitude of which should be quite similar for XPS and XAS. Increases in the C 1s width above the intrinsic value therefore provide information on the bonding interaction of C_{60}. Depending on the system in question, this extra broadening in principle reflects a combination of the following effects: C atomic sites with significantly different environments; creation of electron-hole pairs; coupling to the charge carrier plasmon. The latter two are dominant in cases involving significant charge transfer, such as C_{60}/Ag(111) shown here, for which EELS data [118] show a high intensity of low-energy electronic excitations and the charge carrier plasmon at 0.9 eV. We note that in the C 1s lineshape the coupling to the charge carrier plasmon is difficult to resolve. Typical for the covalently bound MLs in which little or no charge transfer occurs (such as C_{60}/Pt(111) shown here) are narrow C 1s lines. This observation tends to rule out a significant role for inequivalent C sites, which can be tentatively explained by the very efficient intramolecular screening of local charges, as calculated explicitly for a core hole [41].

A further source of information is the shake-up structure, blown up in the right panel of Fig. 14 [1,115]. This structure corresponds to core-ionised final states in which a valence electron is promoted
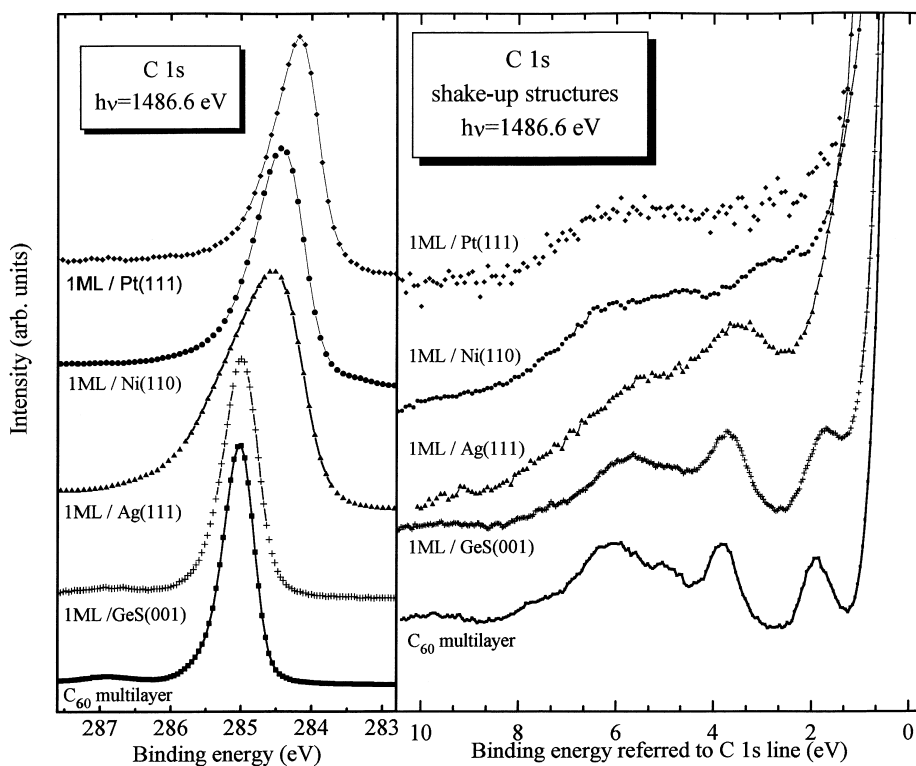
Fig. 14. PES spectra [1,115] of the C 1s core level for a multilayer of C_{60} on GeS(001), and for 1 ML C_{60} on GeS(001), Ag(111), Ni(110) and Pt(111), respectively. The right panel shows an enlargement of the shake-up region for the same samples.

from an occupied to an unoccupied level [49,50], and is therefore similar to a convolution of the occupied and unoccupied parts of the valence band. For the C_{60} ML on GeS one sees only these very sharp intrinsic shake-up structures while in the multilayer extrinsic losses of the outgoing photoelectron produce additional structures in the same energy range [113]. The broadening of the shake-up structures in the other ML films can be regarded as a measure for the bonding interaction with the substrate. On Ag(111), similarly to that on Au(110) [89] and Al(110) [2], the shake-up features are still rather sharp and an intermediate bond strength is deduced. For the C_{60} ML adsorbed on Ni(110) and on Pt(111), the shake-up structures are nearly totally washed out, pointing to an increased bonding inter-action, identifiable with a more covalent character of the bond. A markedly increased broadening has also been reported also for C_{60} MLs on Al(111) [2] and Cr [119] which, based on this criterion of bond

strength, should fall in between C_{60}/Ag(111) and C_{60}/Ni(110) or Pt(111). The same trends were observed in the EELS spectra [118,120] and XAS [2,89], which probe the electronic excitations. How-ever, for the C_{60} ML on all three metal surfaces shown here, the energy positions of EELS peaks and shake-up structures do not coincide, testifying to the influence of the core-hole.

PES [89,121], XAS [89] and EELS [121] experi-ments have also demonstrated that in the case of chemisorption on a noble metal substrate, the in-fluence of the substrate is always limited to the first adsorbed layer of molecules. The thermal stability of adsorbed C_{60} on metal surfaces has been explored by PES, IPES, EELS and AES by following the dis-appearance of the fingerprint of the C_{60} electronic structure and the appearance of that of decomposi-tion products after both long-term annealing [98,99,120,122,123] and nanosecond UV pulsed laser irradiation [124]. In the latter case it was found that

on transition metal surfaces like Ni(111), the chemisorptive bond ensures effective energy dissipation into the substrate and therefore allows the molecule to resist surface temperatures up to 2500 K for a very short time [124]. Long-term annealing experiments showed that coverages above 1 ML desorb at 455 K, while the chemisorbed first layer C_{60} desorbs molecularly from noble metal surfaces like Ag(111) at 670 K [98,99]. On more reactive surfaces decomposition of the molecule is observed at temperatures as low as 690 K and 560 K on Pt(111) and Ni(110), respectively, and this catalytic process is found to be a kinetically-limited reaction [122].

High resolution EELS in reflection has been used for a quantitative estimate of charge transfer from a noble or transition metal substrate to C_{60} based on the shift of the vibrational frequencies [118,120,125]. These measurements have shown that the charge state of the adsorbed fullerene (about 1 electron transferred on Au and Ag, about 2 electrons on Ni) is strongly dependent on the type of metal but rather independent of the work function. The assignments of charge state were given qualitative support by the electronic excitations in the overlayers measured by EELS [118,120,125], which also clearly confirmed the metallic character of the overlayers previously deduced from PES and XAS data [89]. Alternatively, the charge transfer has also been estimated from valence band PES where it manifests itself in the appearance of new LUMO-derived spectral features close to the Fermi edge. For C_{60} MLs on Ag(111) and on polycrystalline Au, Ag and Cu this LUMO-derived intensity was normalised to the areas beneath the MO structures at higher binding energies after subtraction of the clean substrate signal and a charge transfer of about 1.8 ± 0.2 electrons per C_{60} molecule on Cu, 1.7 ± 0.2 on Ag (0.75 on Ag(111)) and 1.0 ± 0.2 on Au was deduced [98,99]. Although these values agree with those deduced from vibrational EELS, this procedure, which relies on the subtraction of the clean substrate signal for quantification of the 'pure' adsorbate signal, is questionable since hybridisation of C_{60} MOs with substrate electronic states is important as pointed out by the authors of Ref. [98,99], and explained above.

As seen in Section 4 for intercalated bulk compounds of C_{60}, higher charge states can be achieved

by reacting the fullerene with alkali metals and this is true also for an adsorbed C_{60} ML. Fig. 15 shows high resolution EELS data for a C_{60} ML deposited on various coverages of Cs on a Au(110) surface: one clearly sees large shifts of C_{60}'s vibrational frequencies when the gold surface is pre-dosed with Cs [36]. By calibrating these shifts against the values for bulk A_xC_{60} compounds [126–128], it has been possible to demonstrate that in the two-dimensional A_xC_{60} overlayers (A=K,Cs) one obtains distinct phases with charge states of approximately 3^-, 4^- and 6^- (depending on the amount of alkali present) and that no intermediate charge states are formed [36,125]. The similarity in electronic structure between the two- and three-dimensional compounds is confirmed by the comparison shown in Fig. 16 of the electronic transitions measured by EELS in reflection (top panels) and the valence band photoemission
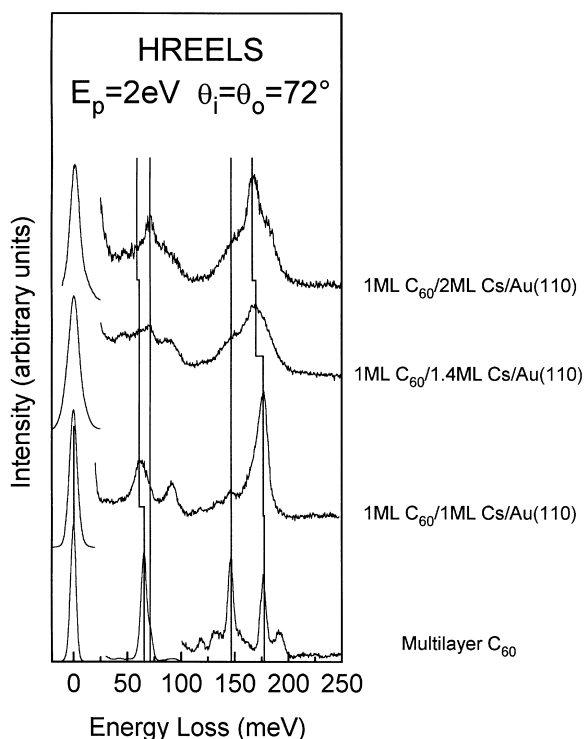

Fig. 15. High resolution EELS spectra measured in reflection in the specular geometry from C_{60} MLs adsorbed on Au(110) with different Cs pre-coverages. The spectrum from an undoped 5 ML C_{60} film is shown at the bottom for comparison. All spectra are normalised to the elastic peak intensity [36].
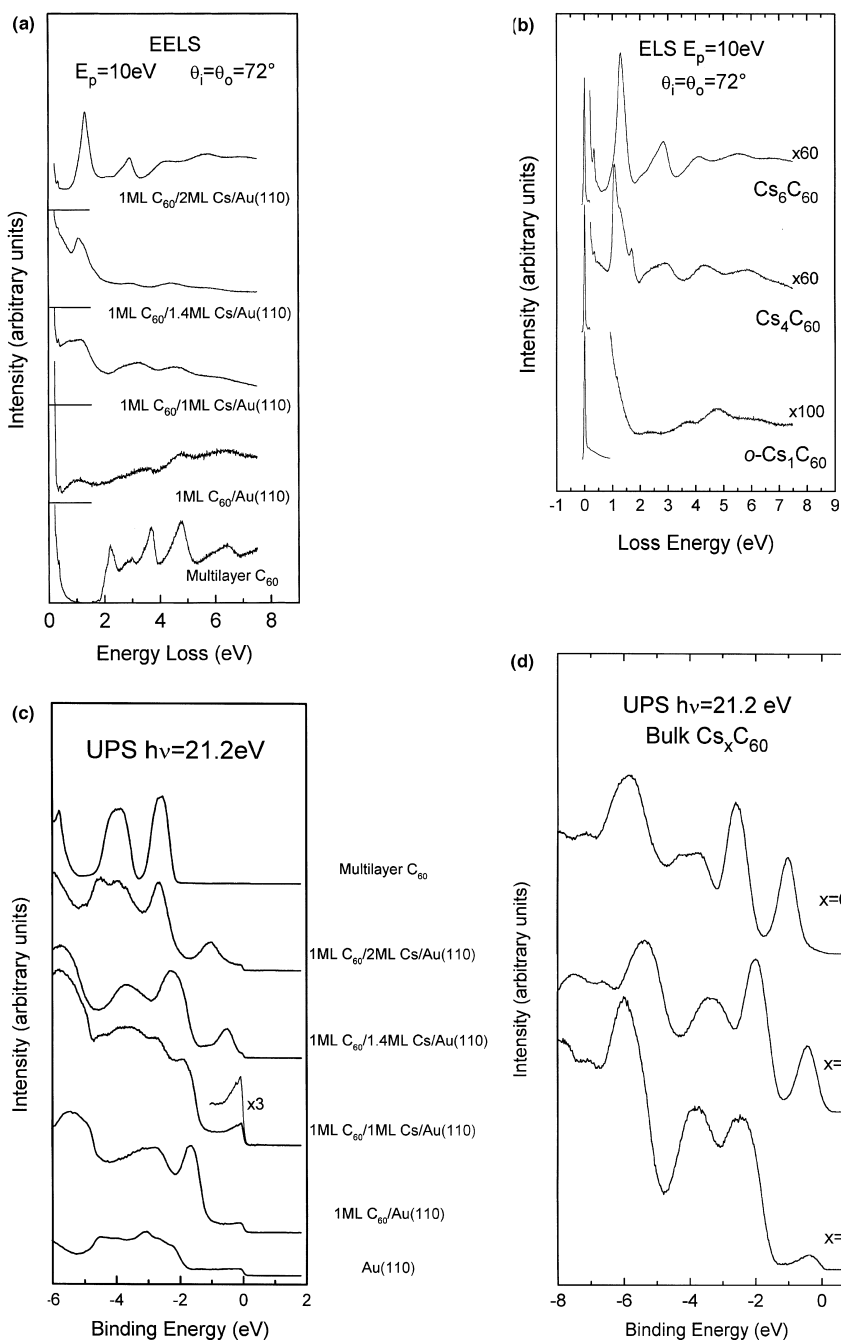
Fig. 16. (a) EELS spectra showing the evolution of the electronic transitions of a ML C_{60} adsorbed on a Cs-pre covered Au(110) surface as a function of Cs coverage. The spectrum from an undoped 5 ML C_{60} film is shown at the bottom for comparison. The solid lines are the zero levels of the spectra. (b) EELS spectra from phase-pure vacuum distilled CsC_{60}, Cs_4C_{60} and Cs_6C_{60} samples. (c) Valence band PES from C_{60} MLs adsorbed on a Cs-precovered Au(110) surface as a function of Cs coverage and normalised to the HOMO-derived peak height. The PES spectra of a bare Au(110) surface and of a C_{60} multilayer are shown at the bottom and the top, respectively, for comparison. (d) Valence band PES from phase-pure vacuum distilled CsC_{60}, Cs_4C_{60} and Cs_6C_{60} samples. The spectra are normalised to the HOMO-derived peak height [36].

(bottom panels) of Cs_4C_{60} and 1 ML C_{60}/1.4 ML Cs/Au(110) or Cs_6C_{60} and 1 ML C_{60}/2 ML Cs/Au(110) [36]. The EELS and valence band PES of 1 ML C_{60}/1 ML Cs/Au(110) should be compared to the K_3C_{60} bulk compound spectra in Figs. 10 and 13, respectively, since pure phase Cs_3C_{60} has not been successfully produced by vacuum distillation so far.

There are, however, some important differences between bulk and surface compounds: in the latter the alkali does not give up its s electron entirely to the fullerene, but there is a competition between charge transfer to the substrate and charge transfer to C_{60}, since a $Cs:C_{60}$ ratio of approximately 4:1 is needed to produce a 3^- charge state in the case of 1 ML C_{60}/1 ML Cs/Au(110). Moreover, if one compares the shifts of the vibrational frequencies in the bulk [126–128] and surface compounds, one notes that except for 1 ML C_{60} on 2 or more MLs of alkali, one of the vibrational modes, the $T_{1u}(4)$ (at 178 meV in the pure C_{60} multilayer) remains 'stiffer' in the surface compounds than in the corresponding bulk compounds as the alkali content increases [36,125] Since theory [129] predicts that molecular distortion is important in determining the softening of this mode, it is likely that this stiffness arises from anisotropies induced in the molecule by bonding to the substrate. Another important difference is that while for bulk compounds the A_4C_{60} phase is the thermodynamically most stable one [78,79], it is the surface compound corresponding a 3^- charge state which is stabilised by the interaction with the substrate. In fact, EELS and PES data have shown that this phase can also be produced by annealing Cs_1C_{60} or Cs_4C_{60} multilayers on Au(110) to 800 K and AES measurements showed that it desorbs stoichiometrically above 900 K [36]. This desorption behaviour suggests that the substrate may form a chemical bond with both the Cs adatoms and the C_{60} in this phase. The formation of A_xC_{60} surface compounds is obviously not unique to the co-deposition of C_{60} and alkalis on Au(110) but has been followed by valence band PES [98,99,130] and IPES [130] also for K-doped monolayers on Ag(111) and on polycrystalline Cu, Ag and Au. Again the surface compound with the 3^- charge state was found to be the most stable [98,99].

The important question as to how the on-site Coulomb interaction, U, is influenced by the prox-imity of a metal has been investigated [130] by measuring the valence band PES spectra for an undoped and a fully K-doped C_{60} ML on Ag(111) and the IPES spectra for the undoped C_{60} ML. For the undoped C_{60} ML the energy separation of the HOMO in electron removal and the LUMO in electron addition is ~2.2 eV [130] (peak to peak), which is a strongly reduced value compared to that of C_{60} bulk and bulk compounds quoted in Sections 3 and 4 above (see Figs. 3, 4 and 12). From the PES of the fully K-doped monolayer, an energy difference between the HOMO- and LUMO-derived peaks, $\Delta=1.6$ eV [130] has been deduced, which is the same as in bulk K_6C_{60} (see Fig. 7 above [69]) and very close to that in other A_xC_{60} bulk compounds (see for example Fig. 16 above [88], and Refs. [95,103,104]), showing that Δ is quite insensitive to the chemical environment and to the charge state of the molecule [130]. From the difference $E_g-\Delta$, U for the surface compound has been determined to be 0.6 eV [130]. A similar analysis of PES [1] and IPES [37] data of 1 ML C_{60}/Au(110) gives $U=2.1$ eV-1.6 eV$=0.5$ eV. This reduction has been explained in terms of screening from the metal [130]. These authors point out that such a screening mechanism due to the proximity of a metal surface is by no means unique to fullerene/metal interfaces but should also strongly modify the electronic structure of correlated ionic insulators at their interface with a metal. We point out, however, that this analysis neglects the chemical bond and the charge transfer between the C_{60} molecule and the substrate while it has been shown that a consequence of this bond is that C 1s binding energy coincides with the XAS threshold indicating metallic screening [89].

6. Exotics/other doping routes

In this section, we move away from C_{60}, aiming to give an impression of the wealth of somewhat more exotic systems to which the fullerene family plays host. Fig. 17 illustrates schematically the three types of doping strategy available for the modification of the electronic structure and properties of fullerenes: exohedral doping (intercalation), on-ball doping (heterofullerene formation) and in-ball doping (endo-hedral fullerene formation). Exohedral doping has

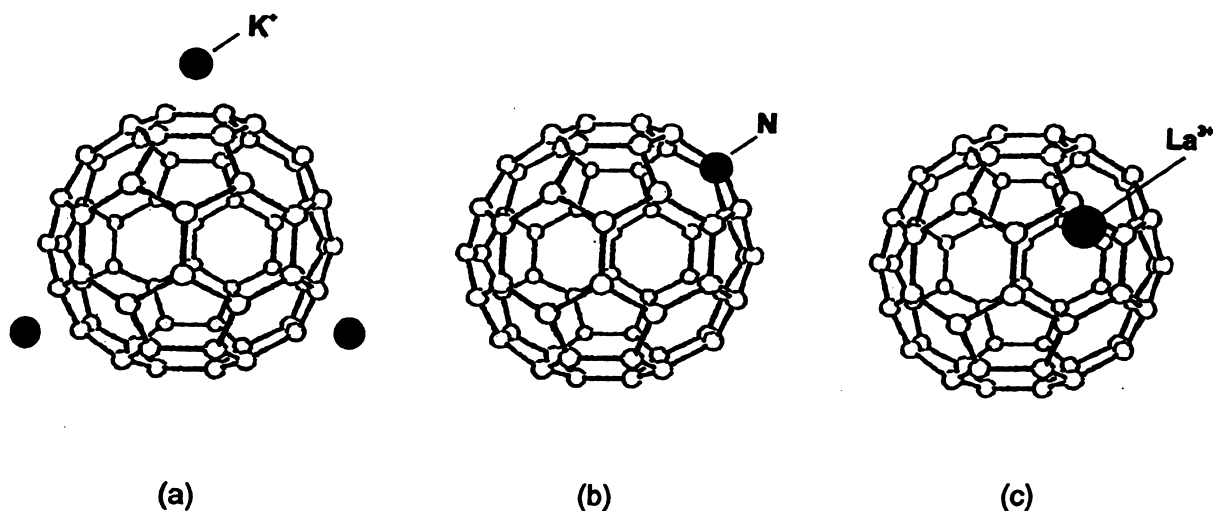**(a)**   **(b)**   **(c)**

Fig. 17. Schematic representation of three possible doping routes in fullerenes.

been dealt with already in Sections 4 and 5, thus we concentrate here on the two remaining doping methods, both of which involve moving away from the 'all carbon' standpoint. The insights offered by electron spectroscopies into the similarities and differences between these systems and C_{60} forms the basis of this section.

The first heterofullerene to be synthesised in macroscopic quantities is $C_{59}N$, or azafullerene [131]. In this system a carbon atom has been replaced by N – a situation formally equivalent to n-type doping. In the solid state, $C_{59}N$ forms dimers which condense in a monoclinic crystal structure [132]. Fig. 18 shows a comparison of the valence band PES and the C 1s excitation spectra (measured using EELS) of $(C_{59}N)_2$ and C_{60} [133]. Also shown is diazafullerene's N 1s excitation spectrum downshifted in energy by 115.5 eV ($=BE_{N1s}-BE_{C1s}$) [134]. At the bottom of each panel are plotted broadened calculated N-derived partial DOS (PDOS) and the total DOS, which were obtained from calculations based upon density functional theory [133,135], shifted such that the energy of the leading maximum matches that observed in experiment. For $(C_{59}N)_2$, both the PES and C 1s excitation spectra are broader than those of C_{60}, but the energy positions of the main features remain essentially unchanged – a result of the lower molecular symmetry. Additionally, the first photoemission maximum
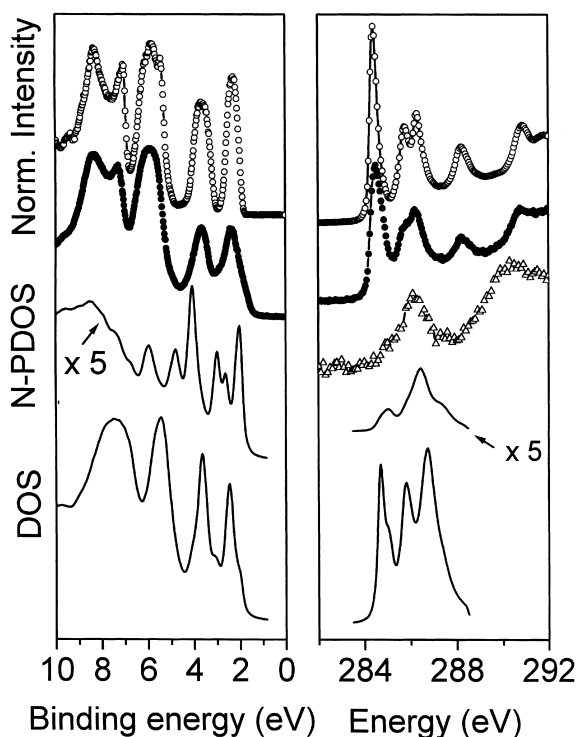

Fig. 18. PES and core level excitation spectra [133] measured using transmission EELS of multilayers of C_{60} and $(C_{59}N)_2$: [○] – pure C_{60}; [●] – $(C_{59}N)_2$; [△] – N 1s excitation of $(C_{59}N)_2$ shifted as described in the text. The solid lines show both the calculated total DOS of $(C_{59}N)_2$, as well as that projected onto the N atomic wave functions.

of $(C_{59}N)_2$ has a shoulder at about 0.5 eV lower BE, which can be assigned to states related to the extra electron which maintains a high degree of nitrogen character. This conclusion is in perfect agreement not only with the N 2p-PDOS, but also with the C 1s and N 1s excitation spectra. Not only is the overall shape of the C 1s excitation spectrum of the heterofullerene very similar to that of C_{60}, the spectral weight of all π^*-derived structures is in fact identical for both systems. This indicates that the N-substitution does not lead to significant occupation of the C-derived low-lying unoccupied states of C_{60}, in agreement with the calculated unoccupied C-PDOS. These results are a direct consequence of the electron density distribution of the HOMO and the LUMO of the $C_{59}N$ dimer. The HOMO of $(C_{59}N)_2$ is very different from that of C_{60} and also from that of a single $C_{59}N$ molecule [136], being strongly concentrated on the N atoms and the intermolecular bond [133,135]. In contrast, the LUMO of $(C_{59}N)_2$ has strong weight on the C atoms sitting at opposite ends of the dimer with only a weak amplitude at the intermolecular bond. EELS investigations of $(C_{59}N)_2$ indicate that the optical gap (1.4 eV) is smaller than that of C_{60} [137,138], in good agreement with Kohn-Sham calculations of the energy levels [135]. The spectroscopic results show that heterofullerene for-

mation is far from a mere *n*-type doping of C_{60}, with the altered molecular structure and presence of the extra nuclear charge at the N site both playing a major role in shaping the electronic structure of diazafullerene.

The next 'doping' strategy to be considered is endohedral doping. One of the key parameters of endohedrally doped fullerenes is the charge transfer between the encaged atom and the fullerene molecule. The vast majority of work on monometallofullerenes containing lanthanide ions has discussed charge transfer exclusively in terms of a $M^{3+}@(C_{82})^{3-}$ configuration (i.e. a charge transfer of 3 electrons). However, already early on, core level photoemission data pointed to a degree of covalence in the $La@C_{82}$ system equivalent to that in $LaBr_3$ [139,140], and a more recent RESPES study suggested a La valence state of 2.7^+ [141].

The first example of a purely divalent lanthanide monometallofullerene is $Tm@C_{82}$ [142,143]. This is demonstrated in Fig. 19, where both the Tm 4f X-ray photoemission spectrum of the C_{3v} isomer of $Tm@C_{82}$ as well as the corresponding Tm 4d excitation spectrum are compared to those of Tm metal and to calculations of the Tm 4f multiplet spectra for a Tm^{2+} and a Tm^{3+} ion [144]. Here we have an excellent example of valence-fingerprinting
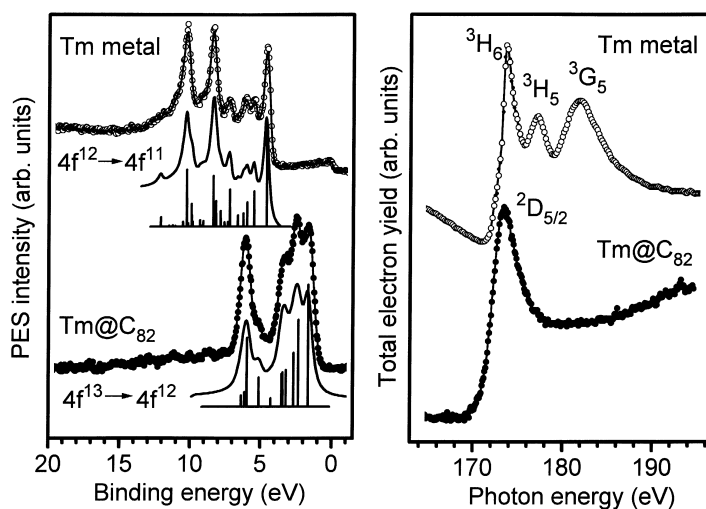

Fig. 19. Left panel: 4f PES spectra [143] of Tm metal and the C_{3v} isomer of $Tm@C_{82}$, accompanied by the appropriate multiplet distributions for photoemission from $4f^{12}$ and $4f^{13}$ initial state configurations, respectively. Right panel: Tm 4d XAS spectra of the corresponding samples.

via the characteristic multiplets in the PES and EELS in transmission spectra. The almost perfect agreement between the endohedral fullerene's Tm 4f PES spectrum and the calculations for a $4f^{13} \to 4f^{12}$ photoemission process, together with the single peak in the core-level excitation spectrum prove conclusively a Tm $4f^{13}$ ground state configuration and thus the pure divalent nature of Tm in Tm@C_{82}. This conclusion is backed up by autoionisation studies (not shown) where even with the photon energy tuned to the energy of one of the Tm(III) $4d \to 4f$ excitation channels, no emission corresponding to a $4f^{11}$ final state is observed. Unlike other systems containing Tm^{2+}, the divalent Tm state in the endohedral fullerene is highly stable, both in UHV and even in air, illustrating the novel properties conferred upon the rare earth ion by its encapsulation within the fullerene molecule.

The last class of fullerenes which we would like to take up are the higher fullerenes and the fullerene polymers. Inevitably, the most widely studied higher fullerene is the next up on the fullerene family-tree from C_{60}: C_{70}, which shares C_{60}'s (experimental) advantage of existing in only a single isomeric form. C_{70} has been investigated in the gas phase [23] as well as in solid form [145], as have its intercalation compounds with the alkali metals K [146] and Rb [5]. Through the comparison between Auger and photoemission data, an estimate of the Coulomb repulsion between two electrons or holes on a single

C_{70} molecule of 1 ± 0.2 eV has been arrived at [145], placing C_{70} in a similar ball-park as C_{60}. Unlike C_{60} though, there have been no spectroscopic (or other) indications of metallic behaviour in any intercalated or otherwise modified C_{70} system. As regards the other higher fullerenes, there have been electron spectroscopic studies of a large number of these, both in their pristine state and intercalated with alkali metals, in which the samples were in the form of a mixture of more than one structural isomer. Under this category fall studies of C_{76} [147–149], C_{78} [149,150], C_{80} [151], C_{82} [149], C_{84} [149,152], and C_{96} [149]. To give a flavour of the trends observed, we show here in Fig. 20 a collection of photoemission and C1s excitation data recorded with EELS in transmission for a range of higher fullerenes.

There is an overall similarity of the occupied and unoccupied electronic states of the fullerenes shown in Fig. 20, which is a natural expression of their common molecular architecture. In general, the energy onset of the C 1s excitation decreases with increasing fullerene size resulting from the decrease in curvature and concurrent decrease of the C 2s contribution to the π-derived states. Noteworthy, however, are the marked differences in the π-derived structures near the chemical potential in the spectra of the two C_{2v} isomers of C_{78} [153], despite the fact that these two molecules differ only by a Stone-Wales transformation (a rotation of one C–C unit by
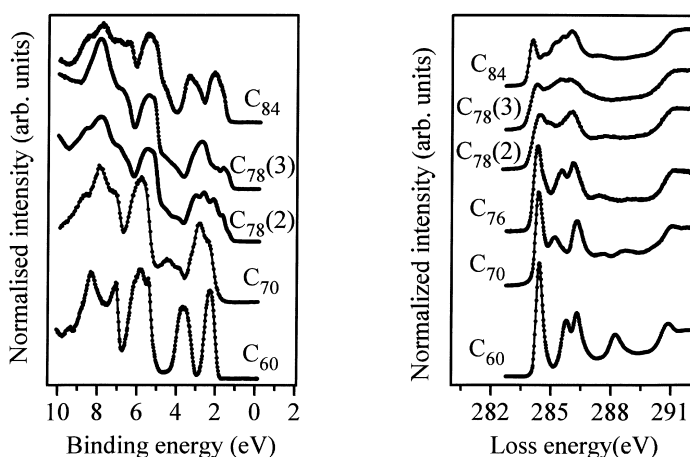

Fig. 20. Left panel: PES spectra of multilayer films of the indicated fullerenes. Right panel: Corresponding C 1s excitation spectra measured using EELS in transmission.

90° [154]). This observation illustrates that even very small variations in the molecular structure have considerable impact on the relative energy position of the lowest lying electronic levels, and underscores the importance of isomer-separated material in the spectroscopic investigation of fullerene-based materials.

7. Summary

We hope we have succeeded in communicating an impression of the numerous valuable insights given by electron spectroscopies in the investigation of the fascinating fullerene family. The intimate connection between structure and electronic properties, which is even more pronounced for molecular or nano-scale objects, suggests that the techniques described here will continue to play an important role as the study of the fullerenes and other carbon-based nanostructures evolves. A relatively underdeveloped component in the electron spectroscopic arsenal which is likely to increase in importance is that of spectroscopy using the scanning tunnelling microscope, as well as the use of higher resolution EELS in the transmission electron microscope. While the latter has been applied so far mainly to carbon nanotubes [155], the former has been used to measure the superconducting energy gap of Rb_3C_{60} [156], and to characterise C_{60} MLs on metals [157–160]. The spatial resolution inherent in these techniques opens new avenues in the investigation of materials as yet unavailable in pure form in macroscopic quantities, thus enabling a more efficient investment of resources in a still rapidly expanding field.

Acknowledgements

References

[1] P. Rudolf, in: H. Kuzmany, J. Fink, M. Mehring, S. Roth (Eds.), Fullerenes and Fullerene Nanostructures, World Scientific, Singapore, 1996, p. 263.

[2] A.J. Maxwell, P.A. Brühwiler, D. Arvanitis, J. Hasselström, M.K.-J. Johansson, N. Mårtensson, Phys. Rev. B57 (1998) 7312.

[3] J.H. Weaver, D. Poirier, in: H. Ehrenreich, F. Spaepen (Eds.), Solid State Physics: Fullerenes, Academic, Boston, 1994, p. 1.

[4] J.H. Weaver, J. Phys. Chem. Solids 53 (1992) 1433.

[5] M.S. Golden, M. Knupfer, J. Fink, J.F. Armbruster, T.R. Cummins, H.A. Romberg, M. Roth, M. Sing, M. Schmidt, E. Sohmen, J. Phys. Condens. Matter 7 (1995) 8219.

[6] D.L. Lichtenberger, M.E. Jatcko, K.W. Nebesny, C.D. Ray, D.R. Huffman, L.D. Lamb, Mat. Res. Soc. Symp. Proc. 206 (1991) 673.

[7] P.A. Brühwiler, A.J. Maxwell, P. Baltzer, S. Andersson, D. Arvanitis, L. Karlsson, N. Mårtensson, Chem. Phys. Lett. 279 (1997) 85.

[8] Taking the centroid of the peak, which is the definition of the vertical ionization potential. The typically-noted value of 7.6 eV refers to the strong peak in the spectrum.

[9] I.V. Hertel, H. Steger, J. deVries, B. Weisser, C. Menzel, B. Kamke, W. Kamke, Phys. Rev. Lett. 68 (1992) 784.

[10] C. Lifshitz, Mass. Spectrom. Rev. 12 (1993) 261.

[11] O. Gunnarsson, H. Handschuh, P.S. Bechthold, B. Kessler, G. Ganteför, W. Eberhardt, Phys. Rev. Lett. 74 (1995) 1875.

[12] We take the centroid of the data of Ref. [11], shown in Fig. 1, and not peak just below 2.70 eV, which corresponds to the adiabatic electron affinity.

[13] L.-S. Wang, J. Conceicao, C. Jin, R.E. Smalley, Chem. Phys. Lett. 182 (1991) 5.

[14] L.-S. Wang, O. Cheshnovsky, R.E. Smalley, J.P. Carpenter, S.J. Hwu, J. Chem. Phys. 96 (1992) 4028.

[15] B. Wästberg, A. Rosén, Phys. Scripta 44 (1991) 276.

[16] T. Liebsch, O. Plotzke, F. Heiser, U. Hergenhahn, O. Hemmers, R. Wehlitz, J. Viefhaus, B. Langer, S.B. Whitfield, U. Becker, Phys. Rev. A52 (1995) 457.

[17] Y.B. Xu, M.Q. Tan, U. Becker, Phys. Rev. Lett. 76 (1996) 3538.

[18] P.A. Brühwiler, A.J. Maxwell, P. Rudolf, C.D. Gutleben, B. Wästberg, N. Mårtensson, Phys. Rev. Lett. 71 (1993) 3721.

[19] Gas phase data at higher temperature, for which vibrational excitation and/or lower resolution obscure some details are given in: S. Krummacher, M. Biermann, M. Neeb, A. Liebsch, W. Eberhardt, Phys. Rev. B48 (1993) 8424.

[20] A.J. Maxwell, P.A. Brühwiler, D. Arvanitis, J. Hasselström, N. Mårtensson, Chem. Phys. Lett. 260 (1996) 71.

[21] P.A. Brühwiler (unpublished).

[22] B. Wästberg, S. Lunell, C. Enkvist, P.A. Brühwiler, A.J. Maxwell, N. Mårtensson, Phys. Rev. B50 (1994) 13031.

[23] R.E. Haufler, L.-S. Wang, L.P.F. Chibante, C. Jin, J. Conceicao, Y. Chai, R.E. Smalley, Chem. Phys. Lett. 179 (1991) 449.

[24] J.W. Keller, M.A. Coplan, Chem. Phys. Lett. 193 (1992) 89.

[25] C. Bulliard, M. Allan, S. Leach, Chem. Phys. Lett. 209 (1993) 434.

[26] R. Abouaf, J. Pommier, S. Cvejanovic, Chem. Phys. Lett. 213 (1993) 503.

[27] A. Burose, T. Dresch, A. Ding, Z. Phys. D 26 (1993) S294.

[28] For theory see K. Yabana, G.F. Bertsch, J. Chem. Phys. 100 (1994) 5580.

[29] A. Bulgac, N. Ju, Phys. Rev. B46 (1992) 4297.

[30] For recent theory and a review, see N. Breda, R.A. Broglia, G. Colò, H.E. Roman, F. Alasia, G. Onida, V. Ponomarev, E. Vigezzi, Chem. Phys. Lett. 286 (1998) 350.

[31] L.-S. Wang, O. Cheshnovsky, R.E. Smalley, J.P. Carpenter, S.J. Hwu, J. Chem. Phys. 96 (1992) 4028.

[32] R.M. Fleming, T. Siegrist, P.M. Marsh, B. Hessen, A.R. Kortan, D.W. Murphy, R.C. Haddon, R. Tycko, G. Dabbagh, A.M. Mujsce, M.L. Kaplan, S.M. Zahurac, Mat. Res. Soc. Symp. Proc. 206 (1991) 691.

[33] P.A. Heiney, J.E. Fischer, A.R. McGhie, W.J. Romanow, A.M. Denenstein, J.P. McCauley, A.B. Smith, D.E. Cox, Phys. Rev. Lett. 66 (1991) 2911.

[34] W.I.F. David, R.M. Ibberson, J.C. Matthewman, K. Prassides, T.J.S. Dennis, J.P. Hare, H.W. Kroto, R. Taylor, D.R.M. Walton, Nature 353 (1991) 147.

[35] However, bond charge interactions have to be invoked as well to account for the stability of the low temperature phase; see for example: J. Yu, L. Bi, R.K. Kalia, P. Vashishta, Phys. Rev. B49 (1994) 5008.

[36] M.R.C. Hunt, P. Rudolf, S. Modesti, Phys. Rev. B55 (1997) 7889.

[37] M. Pedio, M.L. Grilli, C. Ottaviani, M. Capozi, C. Quaresima, P. Perfetti, P.A. Thiry, R. Caudano, P. Rudolf, J. Electron Spectrosc. Related. Phenom. 76 (1995) 405.

[38] R. Schwedhelm, L. Kipp, A. Dallmeyer, M. Skibowski, Phys. Rev. B58 (1998) 13176.

[39] M.B.J. Meinders, L.H. Tjeng, G.A. Sawatzky, Phys. Rev. Lett. 73 (1994) 2937.

[40] R.W. Lof, M.A. van Veenendaal, B. Koopmans, H.T. Jonkman, G.A. Sawatzky, Phys. Rev. Lett. 68 (1992) 3924.

[41] E. Rotenberg, C. Enkvist, P.A. Brühwiler, A.J. Maxwell, N. Mårtensson, Phys. Rev. B54 (1996) R5279.

[42] E.L. Shirley, L.X. Benedict, S.G. Louie, Phys. Rev. B54 (1996) 10970.

[43] P.A. Brühwiler, A.J. Maxwell, A. Nilsson, N. Mårtensson, O. Gunnarsson, Phys. Rev. Rev. B48 (1993) 18296.

[44] R.W. Lof, M.A. vanVeenendaal, H.T. Jonkman, G.A. Sawatzky, J. Electron Spectrosc. Related Phenom. 72 (1995) 83.

[45] P.A. Brühwiler, A.J. Maxwell, N. Mårtensson, Int. J. Mod. Phys. B 6 (1992) 3923.

[46] O. Gunnarsson, D. Rainer, G. Zwicknagl, Int. J. Mod. Phys. B 6 (1992) 3993.

[47] D.P. Joubert, Solid State Commun. 87 (1993) 1009.

[48] G. Gensterblum, K. Hevesi, B.-Y. Han, L.-M. Yu, J.-J. Pireaux, P.A. Thiry, R. Caudano, A.-A. Lucas, D. Bernaerts, S. Amelinckx, G. Van Tendeloo, G. Bendele, T. Buslaps, R.L. Johnson, M. Foss, R. Feidenhans'l, G. Le Lay, Phys. Rev. B50 (1994) 11981.

[49] C. Enkvist, S. Lunell, B. Sjögren, S. Svensson, P.A. Brühwiler, A. Nilsson, A.J. Maxwell, N. Mårtensson, Phys. Rev. B48 (1993) 14629.

[50] C. Enkvist, S. Lunell, B. Sjögren, P.A. Brühwiler, S. Svensson, J. Chem. Phys. 103 (1995) 6333.

[51] E.L. Shirley, S.G. Louie, Phys. Rev. Lett. 71 (1993) 133.

[52] S.G. Louie, E.L. Shirley, J. Phys. Chem. Solids 54 (1993) 1767.

[53] G. Gensterblum, L.-M. Yu, J.-J. Pireaux, P.A. Thiry, R. Caudano, J.P. Vigneron, Ph. Lambin, A.A. Lucas, W. Krätschmer, Phys. Rev. Lett. 67 (1991) 2171.

[54] A. Lucas, G. Gensterblum, J.-J. Pireaux, P.A. Thiry, R. Caudano, J.P. Vigneron, Ph. Lambin, W. Krätschmer, Phys. Rev. B45 (1992) 13694.

[55] E. Sohmen, J. Fink, W. Krätschmer, Europhys. Lett. 17 (1992) 51.

[56] E. Sohmen, J. Fink, Phys. Rev. B47 (1993) 14532.

[57] R. Eder, A.M. Janner, G.A. Sawatzky, Phys. Rev. B53 (1996) 12786.

[58] F. Negri, G. Orlandi, F. Zerbetto, Chem Phys Lett 144 (1998) 31.

[59] C. Cepek, A. Goldoni, S. Modesti, F. Negri, G. Orlandi, F. Zerbetto, Chem. Phys. Lett. 250 (1996) 537.

[60] H. Romberg, E. Sohmen, M. Merkel, M. Knupfer, M. Alexander, M.S. Golden, P. Adelmann, T. Pietrus, J. Fink, R. Seemann, R.L. Johnson, Synth. Met. 55–57 (1993) 3038.

[61] D. Li, S. Velasquez, S.E. Schnatterly, Phys. Rev. B49 (1994) 2969.

[62] A. Goldoni, C. Cepek, S. Modesti, Phys. Rev. B54 (1996) 2890.

[63] K. Zeppenfeld, Z. Phys. 243 (1971) 229.

[64] T. Pichler, M. Knupfer, M.S. Golden, J. Fink, A. Rinzler, R.E. Smalley, Phys. Rev. Lett. 80 (1998) 4729.

[65] P.J. Benning, C.G. Olson, D.W. Lynch, J.H. Weaver, Phys. Rev. B50 (1994) 11239.

[66] G. Gensterblum, J.-J. Pireaux, P.A. Thiry, R. Caudano, T. Buslaps, R.L. Johnson, G. Le Lay, V. Aristov, R. Gunther, A. Taleb-Ibrahimi, G. Indlekofer, Y. Petroff, Phys. Rev. B48 (1993) 14756.

[67] G. Gensterblum, J. Electron Spectrosc. Related Phenom. 81 (1996) 89.

[68] J.-M. Themlin, S. Bouzidi, F. Coletti, J.-M. Debever, G. Gensterblum, L.-M. Yu, J.-J. Pireaux, P.A. Thiry, Phys. Rev. B46 (1992) 15602.

[69] C.-T. Chen, L.-H. Tjeng, P. Rudolf, G. Meigs, J.E. Rowe, J. Chen, J.P. McCauley, A.B. Smith, A.R. McGhie, W.J. Romanow, E.W. Plummer, Nature 352 (1991) 603.

[70] A.J. Maxwell, P.A. Brühwiler, S. Andersson, N. Mårtensson, P. Rudolf, Chem. Phys. Lett. 247 (1995) 257.

[71] W. Andreoni, P. Giannozzi, J.F. Armbruster, M. Knupfer, J. Fink, Europhys. Lett. 34 (1996) 699.

[72] W. Andreoni, P. Giannozzi, M. Parrinello, Phys. Rev. Lett. 72 (1994) 848.

[73] Y. Chen, D.M. Poirier, M.B. Jost, C. Gu, T.R. Ohno, J.L. Martins, J.H. Weaver, L.P.F. Chibante, R.E. Smalley, Phys. Rev. B46 (1992) 7961.

[74] G.K. Wertheim, G.N.E. Buchanan, J.E. Rowe, Science 258 (1992) 1638.

[75] H.A. Romberg, M. Roth, J. Fink, Phys. Rev. B49 (1994) 1427.

[76] M. Knupfer, F. Stepniak, J.H. Weaver, Phys. Rev. B49 (1994) 7620.

[77] D.M. Poirier, Appl. Phys. Lett. 64 (1994) 1356.

[78] D.M. Poirier, J.H. Weaver, Phys. Rev. B47 (1993) 10959.

[79] D.M. Poirier, D.W. Owens, J.H. Weaver, Phys. Rev. B51 (1995) 1830.

[80] M. Knupfer, J.F. Armbruster, H.A. Romberg, J. Fink, Synth. Met. 70 (1995) 1321.

[81] F. Stepniak, P.J. Benning, D.M. Poirier, J.H. Weaver, Phys. Rev. B48 (1993) 1899.

[82] R.F. Kiefl, T.L. Duty, J.W. Schneider, A. MacFarlane, K. Chow, J.W. Elzey, P. Mendels, G.D. Morris, J.H. Brewer, E.J. Ansaldo, C. Niedermayer, D.R. Noakes, C.E. Stronach, B. Hitti, J.E. Fischer, Phys. Rev. Lett. 69 (1992) 2005.

[83] J.P. Lu, Phys. Rev. B49 (1994) 5687.

[84] Y. Iwasa, T. Kaneyasu, M. Nagata, N. Mizutani, Synth. Met. 70 (1995) 1361.

[85] R. Kerkoud, P. Auban-Senzier, D. Jerome, S. Brazovskii, N. Kirova, I. Lukyanchuk, F. Rachdi, C. Goze, Synth. Met. 77 (1996) 205.

[86] M. Knupfer, J. Fink, J.F. Armbruster, Z. Phys. B 101 (1996) 57.

[87] M. Knupfer, J. Fink, Phys. Rev. Lett. 79 (1997) 2714.

[88] M.R.C. Hunt, S. Modesti, M. Pedio, P. Rudolf, unpublished.

[89] A.J. Maxwell, P.A. Brühwiler, A. Nilsson, N. Mårtensson, P. Rudolf, Phys. Rev. B 49 (1994) 10717.

[90] M. Knupfer, J. Fink, J.F. Armbruster, H.A. Romberg, Z. Phys. B 98 (1995) 9.

[91] O. Gunnarsson, V. Eyert, M. Knupfer, J. Fink, J.F. Armbruster, J. Phys.: Condens. Matter 8 (1996) 2557.

[92] A.I. Liechstenstein, O. Gunnarsson, M. Knupfer, J. Fink, J.F. Armbruster, J. Phys.: Condens. Matter 8 (1996) 4001.

[93] V.V. Kresin, V.Z. Kresin, Phys. Rev. B49 (1994) 2715.

[94] M. Knupfer, M. Merkel, M.S. Golden, J. Fink, O. Gunnarsson, V.P. Antropov, Phys. Rev. B47 (1993) 13944.

[95] P.J. Benning, F. Stepniak, D.M. Poirier, J.L. Martins, J.H. Weaver, L.P.F. Chibante, R.E. Smalley, Phys. Rev. B47 (1993) 13843.

[96] G.A. Sawatzky, in: H. Kuzmany, J. Fink, M. Mehring, S. Roth (Eds.), Physics and Chemistry of Fullerenes and Derivatives, World Scientific, 1995, p. 373.

[97] M. Meinders, Ph.D. Thesis, University of Gronginen, 1994.

[98] L.H. Tjeng, R. Hesper, A.C.L. Heessels, A. Heeres, H.T. Jonkman, G.A. Sawatzky, Solid State Commun. 103 (1997) 31.

[99] B.W. Hoogenboom, R. Hesper, L.H. Tjeng, G.A. Sawatzky, Phys. Rev. B57 (1998) 11939.

[100] A. Müller, R. Manzke, P. Rudolf, V. Saltas, in: H. Kuzmany, J. Fink, M. Mehring, S. Roth (Eds.), Fullerenes and Fullerene Nanostructures, World Scientific, Singapore, 1996, p. 298.

[101] D.M. Poirier, C.G. Olson, J.H. Weaver, Phys. Rev. B52 (1995) 11662.

[102] S.L. Molodtsov, C. Casado, M.E. Davila, M. Moreno, F. Soria, M.C. Asensio, J. Phys.: Condens. Matter 6 (1994) 925.

[103] M. De Seta, F. Evangelisti, Phys. Rev. B51 (1995) 6852.

[104] M. De Seta, L. Petaccia, F. Evangelisti, J. Phys.: Condens. Matter 8 (1996) 7221.

[105] A. Gutiérrez, S.L. Molodtsov, J. Phys.: Condens. Matter 9 (1997) 11151.

[106] J. Schnadt, P.A. Brühwiler, N. Mårtensson, F. Rohmund, A. Lassesson, E.E.B. Campbell (unpublished).

[107] J. Fagerström, S. Stafström, Phys. Rev. B53 (1996) 13150.

[108] O. Gunnarsson, Phys. Rev. B51 (1995) 3493.

[109] R. Kerkoud, P. Auban-Senzier, D. Jerome, S. Brazovskii, I. Luk'yanchuk, N. Kirova, F. Rachdi, C. Goze, J. Phys. Chem. Solids 57 (1996) 143.

[110] C.M. Brown, K. Prassides, Y. Iwasa, H. Shimoda, in: K.M. Kadish, R.S. Ruoff (Eds.), Recent Advances in the Chemistry and Physics of Fullerenes and Related Materials, Electrochemical Society, Pennington, NJ, 1997, pp. 1224–1231.

[111] K. Prassides, K. Tanigaki, Y. Iwasa, Physica C 282 (1997) 307.

[112] R.J. Wilson, G. Meijer, D.S. Bethune, R.D. Johnsson, D.D. Chambliss, M.S. de Vries, H.E. Hunziker, H.R. Wendt, Nature 348 (1990) 621.

[113] G. Gensterblum, K. Hevesi, B.Y. Han, L.M. Yu, J.-J. Pireaux, P.A. Thiry, R. Caudano, A.A. Lucas, D. Bernaerts, S. Amelinck, G. Van Tendeloo, G. Bendele, T. Buslaps, R.L. Johnson, M. Foss, R. Feidenhans'l, G. LeLay, Phys. Rev. B50 (1994) 11981.

[114] A.V. Hamza, M. Balooch, Chem. Phys. Lett. 201 (1993) 404.

[115] P. Rudolf, G. Gensterblum, R. Caudano, J. Phys. France 7 (1997) C6–136.

[116] R. Fasel, P. Aebi, R.G. Agostino, D. Namovic, J. Osterwalder, A. Santaniello, L. Schlapbach, Phys Rev. Lett. 76 (1996) 4733.

[117] J.E. Rowe, P. Rudolf, L.H. Tjeng, R.A. Malic, G. Meigs, C.T. Chen, J. Chen, E.W. Plummer, Int. J. Mod. Phys. B6 (1992) 3909.

[118] M.R.C. Hunt, S. Modesti, P. Rudolf, R.E. Palmer, Phys. Rev. B51 (1995) 10039.

[119] T.R. Ohno, Y. Chen, S.E. Harvey, G.H. Kroll, J.H. Weaver, R.E. Haufler, R.E. Smalley, Phys. Rev. B44 (1991) 13747.

[120] C. Cepek, A. Goldoni, S. Modesti, Phys. Rev. B53 (1996) 7466.

[121] M.R.C. Hunt, P. Rudolf, S. Modesti, Phys. Rev. B55 (1997) 7882.

[122] M. Pedio, K. Hevesi, N. Zema, M. Capozi, P. Perfetti, R. Gouttebaron, J.-J. Pireaux, R. Caudano, P. Rudolf, Surface Science, in press.

[123] A. Sellidj, B.E. Koel, J. Phys. Chem. 97 (1993) 10076.

[124] Ch. Kusch, B. Winter, R. Mitzner, A. Gomes-Silva, E.E.B. Cambell, I.V. Hertel, Chem. Phys. Lett. 275 (1997) 469.

[125] S. Modesti, S. Cerasari, P. Rudolf, Phys. Rev. Lett. 71 (1993) 2469.

[126] Y. Iwasawa, T. Kaneyasu, Phys. Rev. B51 (1995) 3678.

[127] T. Pichler, M. Matus, H. Kuzmany, Solid State Commun. 86 (1993) 221.

[128] T. Pichler, R. Winkler, H. Kuzmany, Phys. Rev. B49 (1994) 15879.

[129] P. Giannozzi, W. Andreoni, Phys. Rev. Lett. 76 (1996) 4915.

[130] R. Hesper, L.H. Tjeng, G.A. Sawatzky, Europhysics Lett. 40 (1997) 177.

[131] J.C. Hummelen, B. Knight, J. Pavlovich, R. Gonzales, F. Wudl, Science 269 (1995) 1554.

[132] C.M. Brown, L. Cristofolini, K. Kordatos, K. Prassides, C. Bellavia-Lund, R. Gonzales, M. Keshavarz-K, F. Wudl, A.K. Cheetham, J.P. Zhang, W. Andreoni, A. Curioni, A.N. Fitch, P. Pattison, Chem. Mater. 8 (1996) 2548.

[133] T. Pichler, M. Knupfer, M.S. Golden, S. Haffner, R. Friedlein, J. Fink, W. Andreoni, A. Curioni, M. Keshavarez-K, C. Bellavia-Lund, A. Sastre, J.C. Hummelen, F. Wudl, Phys. Rev. Lett. 78 (1997) 4249.

[134] S. Haffner, T. Pichler, M. Knupfer, B. Umlauf, R. Friedlein, M.S. Golden, J. Fink, M. Keshavarez-K, C. Bellavia-Lund, A. Sastre, J.C. Hummelen, F. Wudl, Eur. Phys. J. B 1 (1998) 11.

[135] W. Andreoni, A. Curioni, K. Holczer, K. Prassides, M. Keshavarz-K, J.C. Hummelen, F. Wudl, J. Am. Chem. Soc. 118 (1996) 11335.

[136] W. Andreoni, F. Gygi, M. Parrinello, Chem. Phys. Lett. 190 (1992) 159.

[137] T. Pichler, M. Knupfer, R. Friedlein, S. Haffner, B. Umlauf, M.S. Golden, O. Knauff, H.D. Bauer, J. Fink, M. Keshavarezk, C. Bellavia-Lund, A. Sastre, J.-C. Hummelen, F. Wudl, Synth. Met. 86 (1997) 2313.

[138] T. Pichler, M. Knupfer, M.S. Golden, J. Fink, J. Winter, M. Haluska, H. Kuzmany, M. Keshavarez-K, C. Bellavia-Lund, A. Sastre, J.-C. Hummelen, F. Wudl, Appl. Phys. 64 (1997) 301.

[139] J.H. Weaver, Y. Chai, G.H. Kroll, C. Lin, T.R. Ohno, R.E. Hauffler, T. Guo, J.M. Alford, J. Conceicao, L.P.F. Chibante, A. Jain, G. Palmer, R.E. Smalley, Chem. Phys. Lett. 190 (1992) 460.

[140] D.M. Poirier, M. Knupfer, J.H. Weaver, W. Andreoni, K. Laasonen, M. Parrinello, D.S. Bethune, K. Kikuchi, Y. Achiba, Phys. Rev. B49 (1994) 17403.

[141] B. Kessler, A. Bringer, S. Cramm, C. Schlebusch, W. Eberhardt, S. Suzuki, Y. Achiba, F. Esch, M. Barnaba, D. Cocca, Phys. Rev. Lett. 79 (1997) 2289.

[142] U. Kirbach, L. Dunsch, Angew. Chem. Int. Ed. Engl. 35 (1996) 2380.

[143] T. Pichler, M.S. Golden, M. Knupfer, J. Fink, U. Kirbach, P. Kuran, L. Dunsch, Phys. Rev. Lett. 79 (1997) 3026.

[144] F. Gerken, J. Phys. F 13 (1983) 703.

[145] M. Knupfer, D.M. Poirier, J.H. Weaver, Phys. Rev. B49 (1994) 2281.

[146] M. Knupfer, D.M. Poirier, J.H. Weaver, Phys. Rev. B49 (1994) 8464.

[147] S. Hino, K. Matsumoto, S. Hasegawa, H. Inokuchi, K. Seki, K. Kikuchi, S. Suzuki, I. Ikemoto, Y. Achiba, Chem. Phys. Lett. 197 (1992) 38.

[148] J.F. Armbruster, H.A. Romberg, P. Schweiss, P. Adelmann, M. Knupfer, J. Fink, R.H. Michel, J. Rockenberger, F. Hennrich, H. Schreiber, M.M. Kappes, Z. Phys. B 95 (1994) 469.

[149] S. Hino, K. Kikuchi, Y. Achiba, Synth. Met. 70 (1995) 1337.

[150] S. Hino, H. Takahashi, K. Iwasaki, T. Miyazaki, K. Kikuchi, Y. Achiba, Chem. Phys. Lett. 230 (1994) 165.

[151] T.R. Cummins, M. Bürk, M. Schmidt, J.F. Armbruster, D. Fuchs, P. Adelmann, S. Schuppler, R.H. Michel, M.M. Kappes, Chem. Phys. Lett. 261 (1996) 228.

[152] J.F. Armbruster, M. Roth, H.A. Romberg, M. Sing, M. Schmidt, P. Schweiss, P. Adelmann, M.S. Golden, J. Fink, R.H. Michel, J. Rockenberger, F. Hennrich, M.M. Kappes, Phys. Rev. B50 (1994) 4933.

[153] M. Knupfer, O. Knauff, M.S. Golden, J. Fink, M. Bürk, D. Fuchs, S. Schuppler, R.H. Michel, M.N. Kappes, Chem. Phys. Lett. 258 (1996) 513.

[154] A.J. Stones, D.J. Wales, Chem. Phys. Lett. 128 (1986) 501.

[155] See for example: N. Demoncy, O. Stéphan, N. Brun, C. Colliex, A. Loiseau, H. Pascard, Euro. Phys. J. B4 (1998) 147.

[156] Z. Zhang, C.-C. Chen, S.P. Kelty, H. Dai, C.M. Lieber, Nature 353 (1991) 33.

[157] J.K. Gimzewski, S. Modesti, C. Gerber, R.R. Schlittler, Chem. Phys. Lett. 213 (1992) 401.

[158] Y. Kuk, D.K. Kim, Y.D. Suh, K.H. Park, H.P. Noh, S.J. Oh, S.K. Kim, Phys. Rev. Lett. 70 (1993) 1948.

[159] E.I. Altman, R.J. Colton, Phys. Rev. B48 (1993) 18244.

[160] M.K.-J. Johansson, A.J. Maxwell, S.M. Gray, P.A. Brühwiler, D.C. Mancini, L.S.O. Johansson, N. Mårtensson, Phys. Rev. B54 (1996) 13472.